Contents of this file

Introduction

The supporting information includes an overview of comparison between three emission inventories and their impact on air quality results (Text S1), a guideline how to use the IRR outputs of WRF-Chem model (Text S2), the method to classify grid cells as urban, rural, or power plant region (Text S3), and figures and tables supporting the results in the main manuscript.

Text S1- Comparing different anthropogenic emission inventories and their impacts on air quality findings

We compared the emissions in three most commonly used global emission inventories that can be applied for regional air quality modeling over India. Specifically, we looked at the total and sectoral emissions of Hemispheric Transport of Air Pollution emission inventory (HTAP v2.2), Copernicus Atmosphere Monitoring Service global emission inventory version 4.2 (CAMS v4.2), and the modified Community Emissions Data System emission inventory (CEDS_M).

HTAP v2.2 is a 0.1x0.1 degree gridded monthly-averaged for each sector for base year of 2010 (Janssens-Maenhout et al., 2015). We used the speciation provided by Emissions of atmospheric Compounds and Compilation of Ancillary Data (ECCAD) database for NMVOCs, which is based on ratios in the RETRO project (https://permalink.aeris-data.fr/HTAPv2, last access: 20 December 2020). Moreover, the mapping between the both ECCAD and CEDS_M NMVOCs and model emitted species are provided in Table S1 (personal communications with Louisa Emmons, NCAR). CAMS v4.2 (available from ECCAD database (https://permalink.aeris-data.fr/CAMS-GLOB-ANT, last access: 02/23/2021) provides 0.1x0.1 degree gridded monthly-averaged emissions for the years between 2000 and 2020. It uses Emissions Database for Global Atmospheric Research version 4.3.2 (EDGARv4.3.2) for the years before 2012 and projects emissions between 2012 and 2020 using the CEDS emission trends (Granier et al., 2019). The information about the CEDS_M, which is the base emission inventory in this study, can be found in the main text.

Figure S27 shows the total and spatial pattern of emissions in April based on each emission inventory. For NOx, the total emissions in HTAP v2.2 and CEDS_M are close together and about 10% lower than in CAMS v4.2. The spatial patterns are also similar between HTAP v2.2 and CEDS_M showing more spread of emissions over the IGP region. However for NMVOCs, CEDS_M and CAMS shows about 40% reduction in emissions compared to HTAP v2.2 although the spatial pattern remained the same. On the other hand, CEDS_M increased both BC and OC emissions by about 20% compared with HTAP v2.2. Another major difference between these two emission inventories for BC and OC is that CEDS_M allocated more emissions over the IGP region. Models with no data assimilation usually have troubles to capture the high $PM_{2.5}$ concentrations using HTAP v2.2 over this region (Roozitalab et al., 2021). This increase could resolve this issue to some extents. The SO_2 and NH_3 emissions are also higher in CEDS_M by 25% and 130% ,respectively, compared with HTAP v2.2. Larger NH_3 emissions are also provided by CAMS v4.2 compared with HTAP v2.2. Although nitrates are not considered currently as a main component of $PM_{2.5}$ over India (Venkataraman et al., 2018), this higher NH_3 emissions, specifically over the IGP region, could affect the thermodynamic equilibrium of the model because of more anions (Vasilakos et al., 2018).

The sectoral allocations in these emission inventories are also different. Figure S28shows the sectoral contribution for each species over India and over the urban pre-defined sub region. For NOx, transport sector is dominant while it is the third ranked sector in CEDS_M. Energy and industry sectors emit more NOx in CEDS_M emission inventory. Energy is also the dominant sector in CAMS v4.2 for NOx emissions. Similarly, transport sector is dominant in HTAP v2.2 over the urban region while industry sector emits more NOx in CEDS_M emission inventory. For NMVOCs, residential sector is the dominant sector in all the inventories when looking at India. Nevertheless, the contribution of transport sector is decreased in CEDS_M and CAMS v4.2 inventories compared with HTAP v2.2 over India. On the other hand, the dominant sector for NMVOCs over the urban region is different. Specifically, transport, industry, and residential sectors are dominant sectors of NMVOCs in HTAP v2.2, CAMS v4.2, and CEDS_M emission inventories, respectively. Although there are some local emission inventories available throughout the country (Guttikunda et al., 2019;Jena et al., 2021), this comparison showed the necessity of an updated gridded national emission inventory for India.

We performed an experiment using HTAP v2.2 emission inventory to see which inventory provides better air quality results over the domain. Table S6 shows that statistics for O_3 MDA8 and daily means for NO_2, and $PM_{2.5}$ concentrations. It should be mentioned

that the results in the main text are based on CEDS_0.75NOXnight_1.25NOXday_0.5BC. CEDS_M and other global inventories do not provide diurnal profile in the emissions (i.e. they are monthly). To account for the diurnal pattern of NOx emissions in the inventory, we perturbed nighttime and daytime emissions by 25%. Although we acknowledge this simplification has large uncertainties (e.g. not all the sectors have diurnal profile for NOx emissions), we found better representation of nighttime NO_2 concentrations. It shows that studies should apply more detailed diurnal profiles in their studies based on more detailed diurnal profiles (e.g. Wang et al. (2014)).

Furthermore, the results in the main text are based on 50% lower ozone from boundary conditions (0.5BC). Therefore, we also provide the statistics for a scenario, where we only switched the emission inventories (columns 1 and 2 in the table). By switching the emission inventories, we significantly improved the NO_2 and $PM_{2.5}$ statistics. However, the results for ozone were slightly degraded (which we eventually could improve by reducing the transboundary ozone from BCs). We decreased the ozone from boundary condition because we found that it affects surface ozone over the domain. Figure S29 Shows the impact of 50 percent higher ozone only in the boundary condition data through a horizontal cross section over the domain after 60 hours; showing about 20ppb higher ozone on the surface. On the other hand, this modification also significantly decreases ozone concentrations in upper levels of the atmosphere. BC ozone is certainly not high on all the layers, but either its vertical profile is not right (WRF interpolates it), or dynamics of the model is not accurate (PBL height measurement can clarify this), or BC ozone amounts in lower levels (in global models) are actually high. The focus of current study was surface ozone formation and changes due to different years but the impacts of transboundary ozone on surface and upper levels should be studied more carefully in future works.

Text S2. Using IRR data in WRF-Chem model

IRR provides the gas-phase reaction rate for the species involved in each reaction. As a simple unit for these outputs, IRR within the WRF-Chem model, are in ppb and are cumulative. As a result, the hourly reaction rates (ppb/hr) can be calculated by subtracting the values in two consecutive hours. We use the difference between hours "i" and "i+1" as the reaction rate in hour "i". Reporting this information in 'ppb/hr' makes the data easy-to-report and useful for all the species within the reaction. For example, in the reaction A+B-> C+D, a single reaction rate of RR in ppb/hr shows that RR ppb of A and B was consumed and RR ppb of C and D was produced in a specific hour. In our analysis, we used the IRR information averaged within the boundary layer following Pfister et al. (2019).

Text S3. Grid classification algorithm

We classified each grid cell as urban, rural, or power-plant, when analyzing the ozone FNR analysis and making general conclusions, based on the list of National Clean Air Programme (NCAP) non-attainment cities and emission information. In particular, we used the shape file of NCAP airsheds to find the cities. It includes 94 airsheds covering 122 non-attainment cities in NCAP over India. However, our analysis is based on the model results and the used emission data did not showed large emissions in all of these airsheds. Thus, we added another filter to check the emissions. As a result, we used the following process for classifying each grid cell. It should be mentioned that the threshold limits have been determined based on analyzing different values. Furthermore, the CEDS_M emissions are used for the classification.

For urban grid cells:

- It should be included in the NCAP cities.
- NOx emission flux in the transportation sector should be equal or more than 1.5 moles/km2/hr. We used 3 moles/km2/hr for HTAP v2.2 emissions since its emissions were larger.

For rural grid cells:

- NOx emission flux in the transportation sector should be less than 1.5 moles/km2/hr.
- SO_2 emission flux in the energy sector should be less than 10 moles/km2/hr.

For power plant grid cells:

- NOx emission flux in the transportation sector should be less than 1.5 moles/km2/hr.
- SO_2 emission flux in the energy sector should be equal or more than 10 moles/km2/hr.

Figure S22 shows the grid cells classification results.
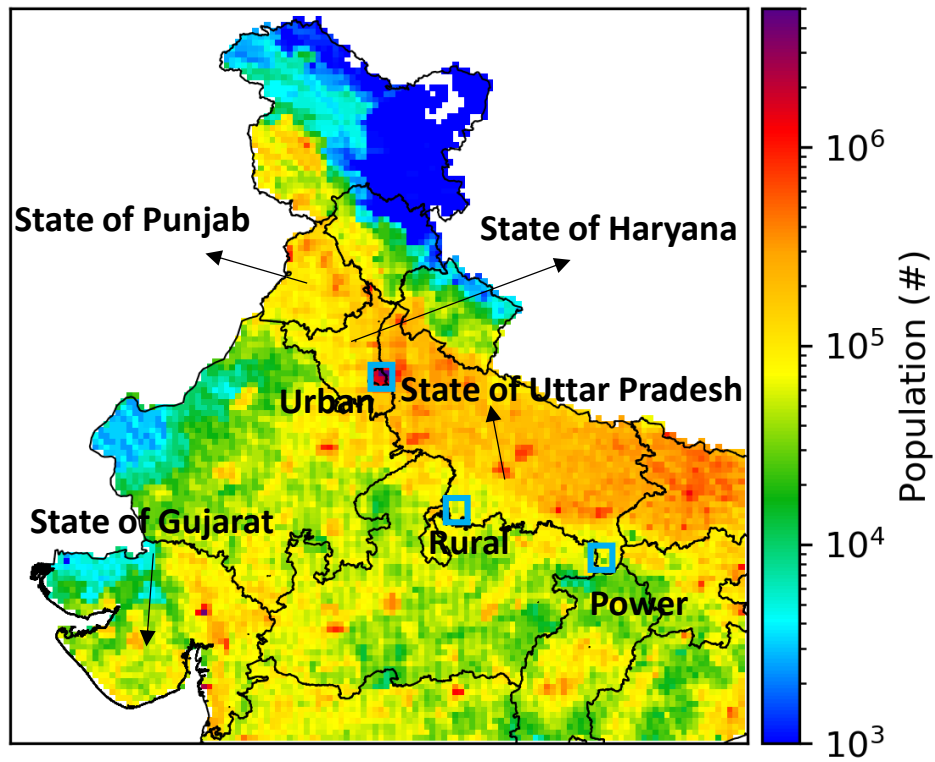
Figure S1 Location of the selected regions of Urban (Lower Left (LL): 28.3N, 76.7E, Upper Right (UR): 28.9N, 77.5E), Rural (LL: 25.1N, 79E, UR: 25.6N, 79.75E), and Power (LL: 23.9N, 82.5E, UR: 24.5N, 83.3E). States of Punjab, Haryana, Uttar Pradesh, and Gujarat are also shown. The background map shows the 2020 population counts based on Global World Population v4 (Center for International Earth Science Information Network - CIESIN - Columbia University, 2018).

a) Total fire emissions

b) Daily emissions ratio (2020/2019)
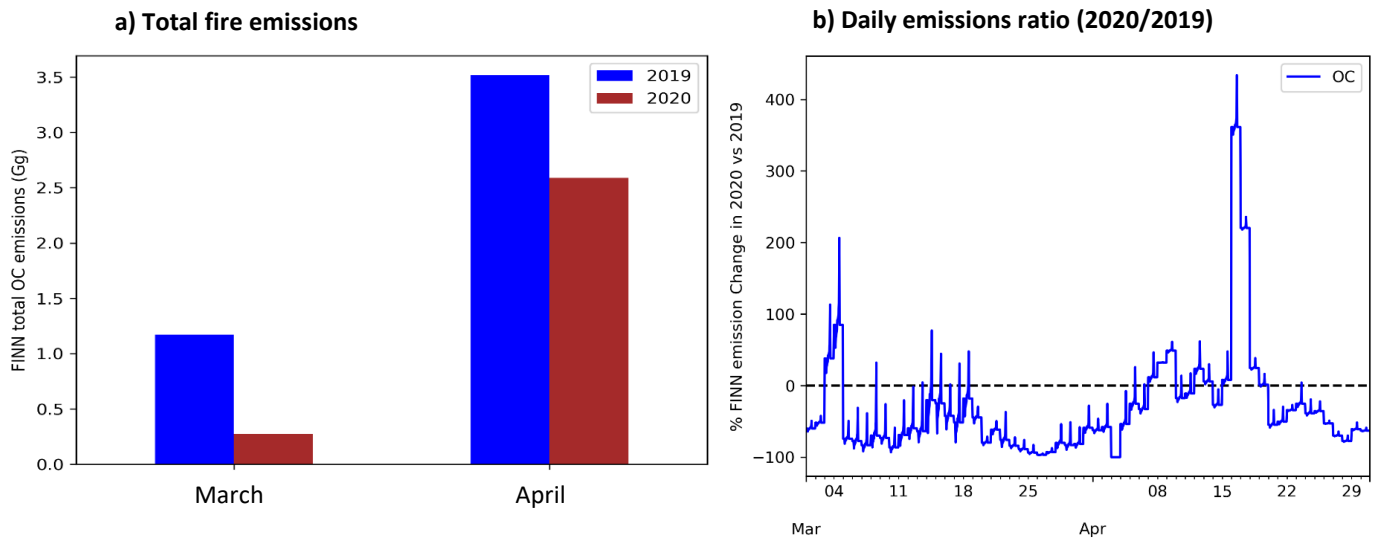
Figure S2 Comparison of FINN biomass burning emissions between 2019 and 2020 for a) total emissions and b) the ratio of daily emissions

7
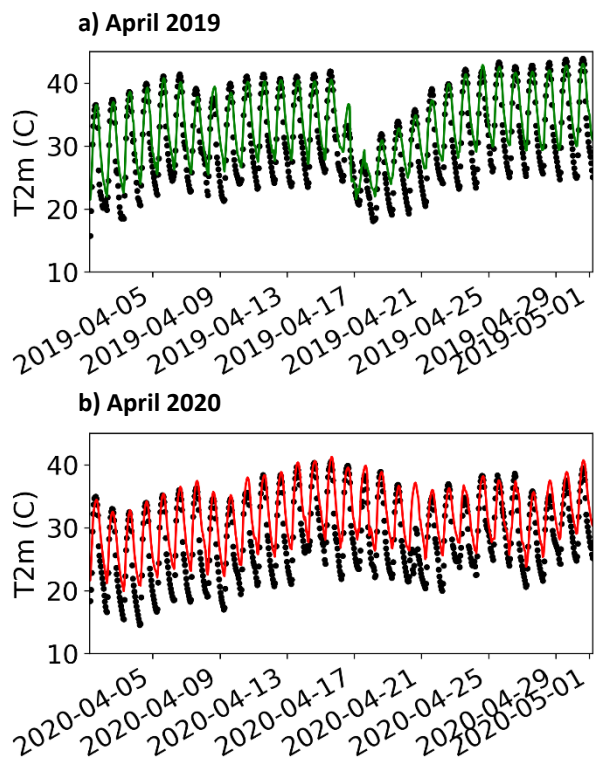
Figure S3 Timeseries of 2m temperature in model (black dots) and MERRA-2 (green line in 2019 (a) and red line in 2020 (b)) in a grid cell over Delhi (28.6N, 77.19 E)

a) April 2019-Model

b) April 2019-MERRA2

c) April 2019-Bias

d) April 2020-Model

e) April 2020-MERRA2

f) April 2020-Bias

g) April 2019
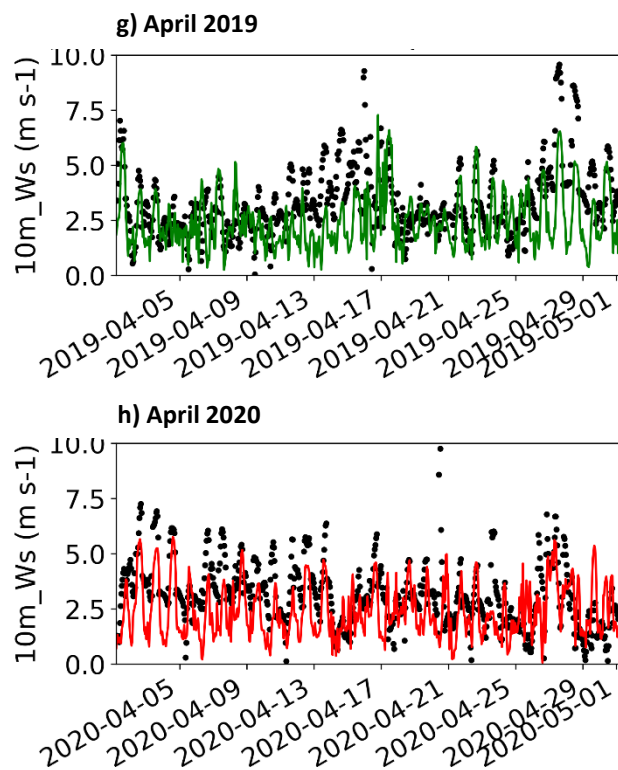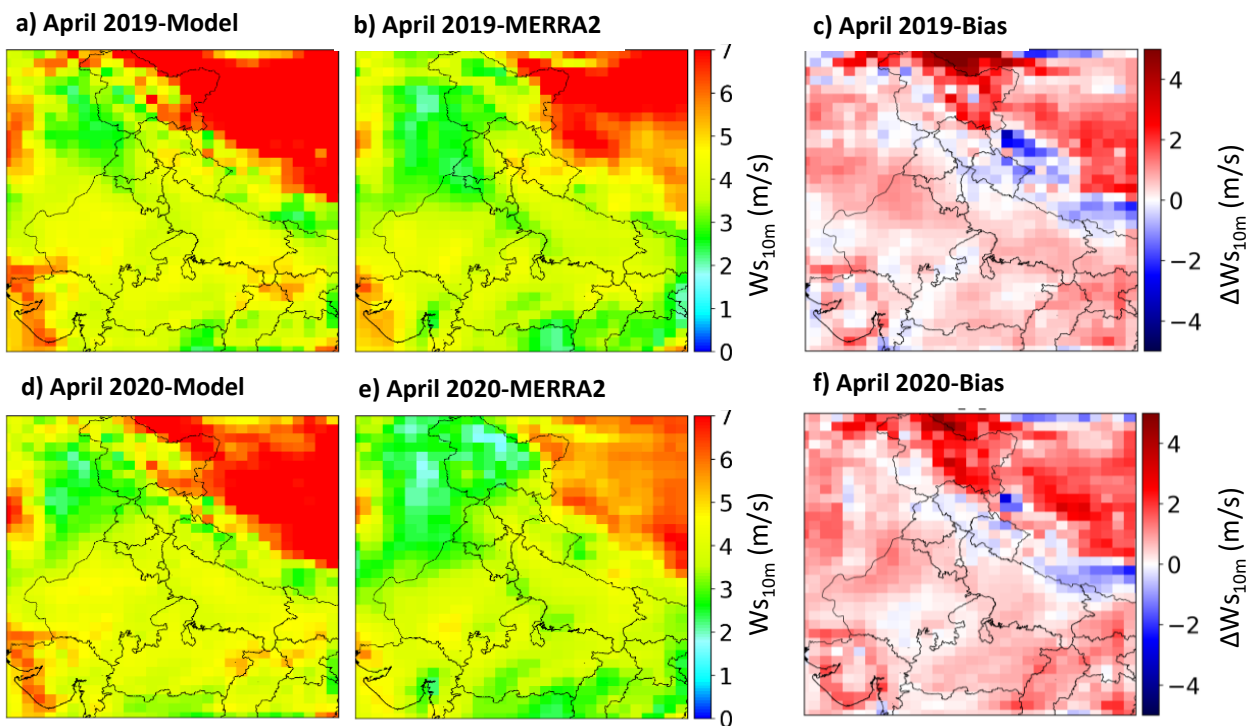
h) April 2020

Figure S4 Temporospatial performance of the model for 10 m wind speed in April 2019 and 2020. Timeseries (g,h) are for a location in Delhi (28.6N, 77.19 E)
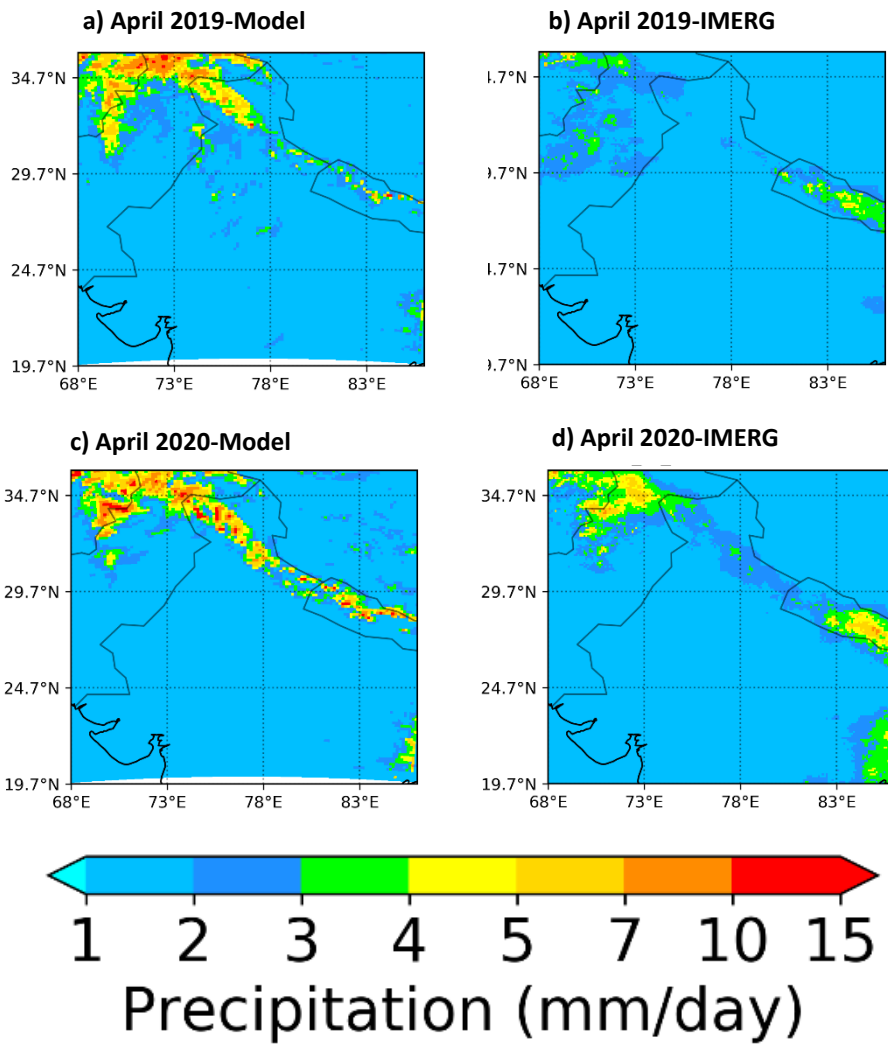
Figure S5 Mean daily modeled (left column) and observed (right column) precipitation in April 2019 (top row) and 2020 (bottom row). Observed data are based on IMERG dataset.
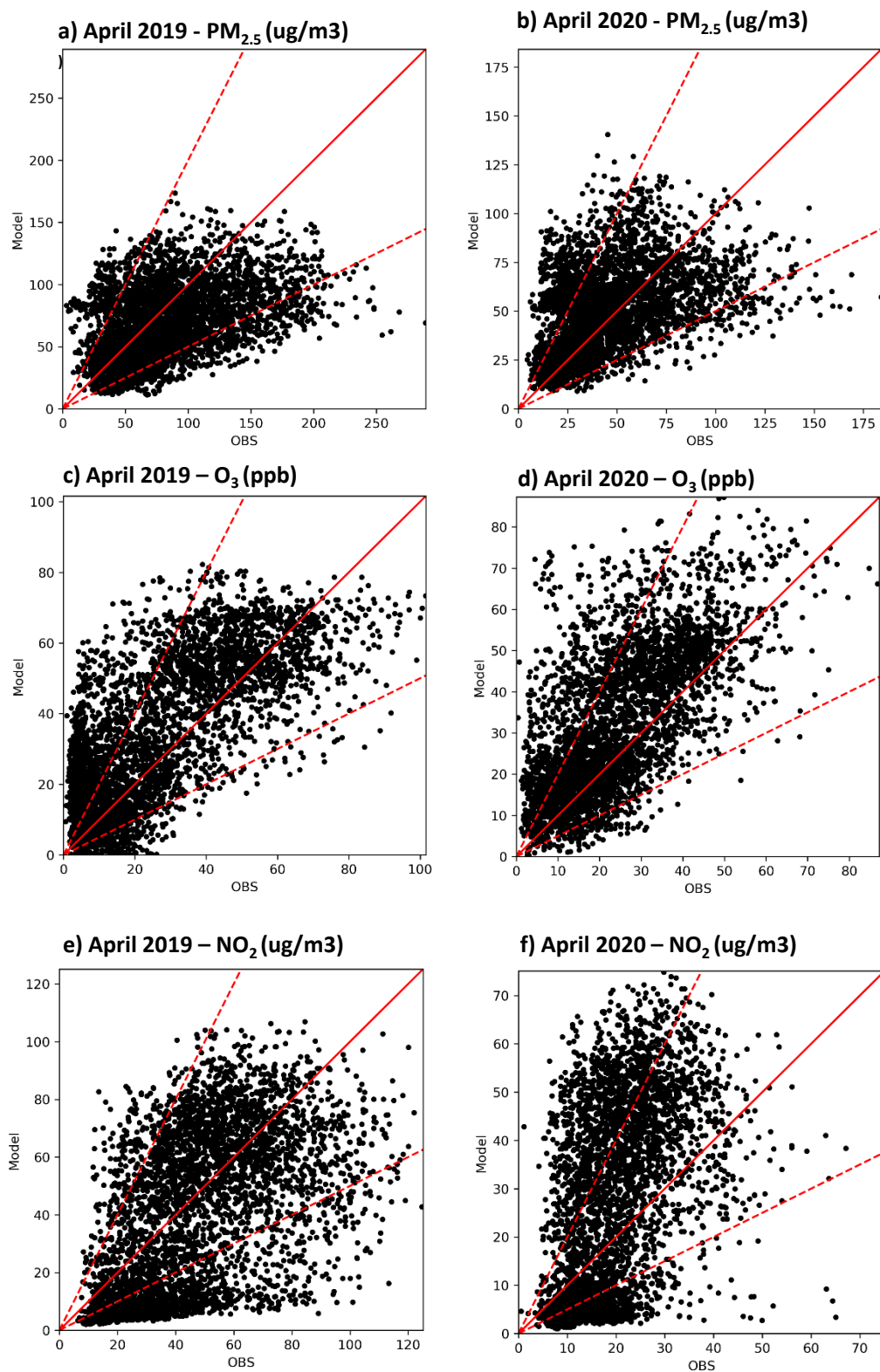
Figure S 6 hourly scatterplots of the modeled vs. ground measurement concentrations of PM$_{2.5}$ (a,b), ozone (c,d), and NO$_2$ (e,f)in During April 2019 and 2020, respectively. The 1:1 line is shown in solid red and 1:2 lines are shown in dashed red lines.
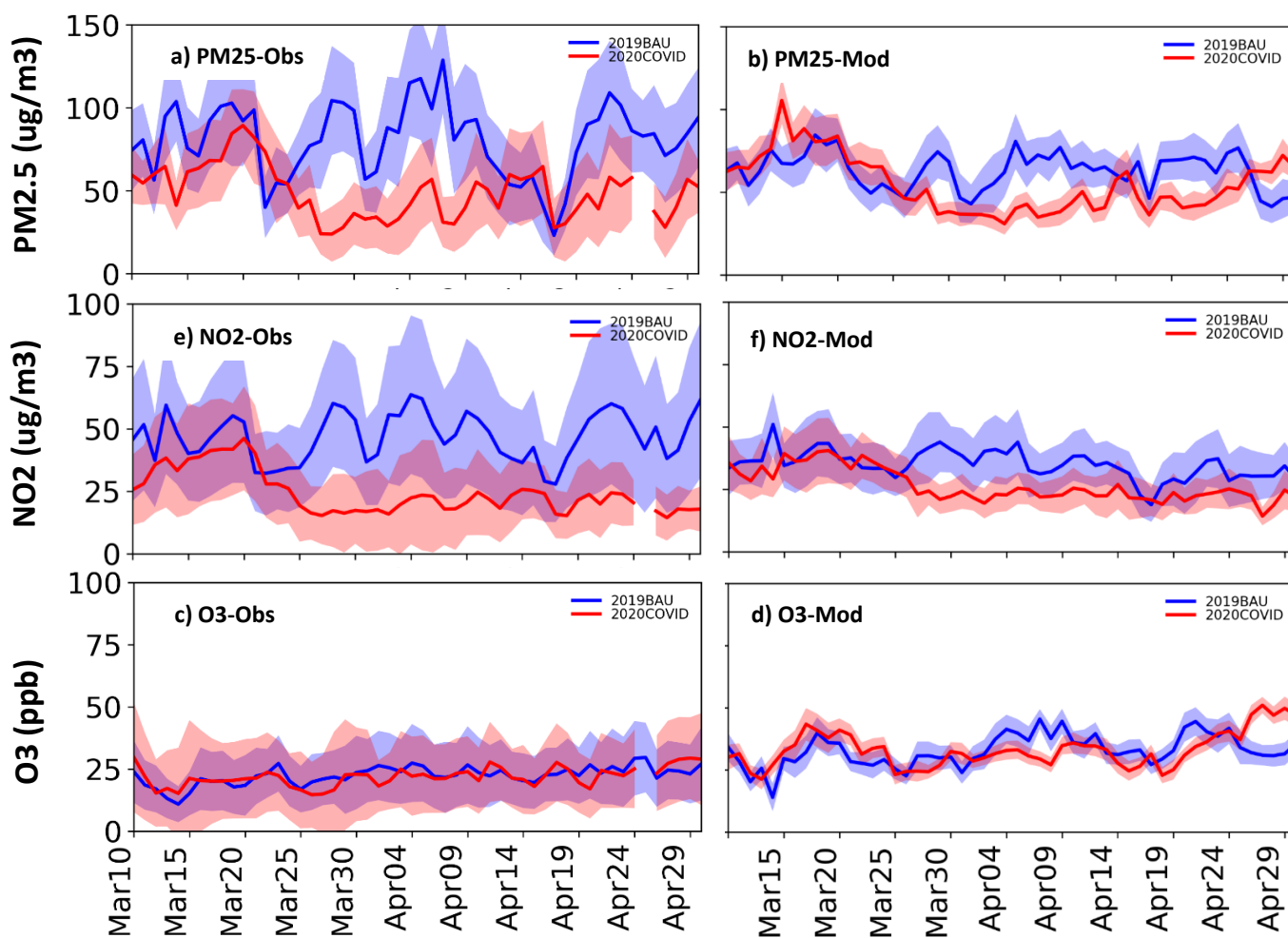
Figure S7 24-hour averaged PM₂.₅ (top row), NO₂ (middle row), and ozone (bottom row) concentrations measured over CPCB stations in Delhi (left column) and modeled over Urban region (right column) between 10 March and 30 April in 2019 (green colors) and 2020 (red colors). The shaded regions show ±1STD. The observed data were extracted from the ground measurements data in Delhi, while the modeled data were averaged in the Urban box region.

a) PM₂.₅

b) NO₂

c) O₃
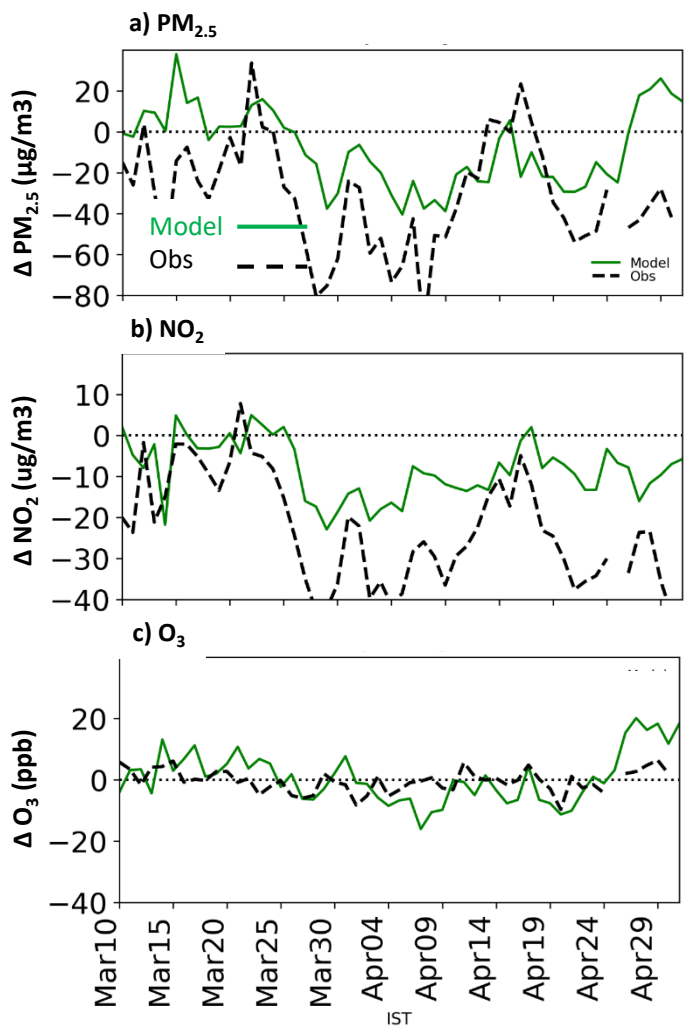
Figure S8 Averaged daily PM₂.₅ (top row), NO₂ (middle row), and ozone (bottom row) concentration changes between 2020 and 2019, during 10 March and 30 April, based on the measured data over CPCB stations in Delhi (black dashed line) and modeled data (green solid line) over Urban region. The observed data were extracted from the ground measurements data in Delhi, while the modeled data were averaged in the Urban box region.
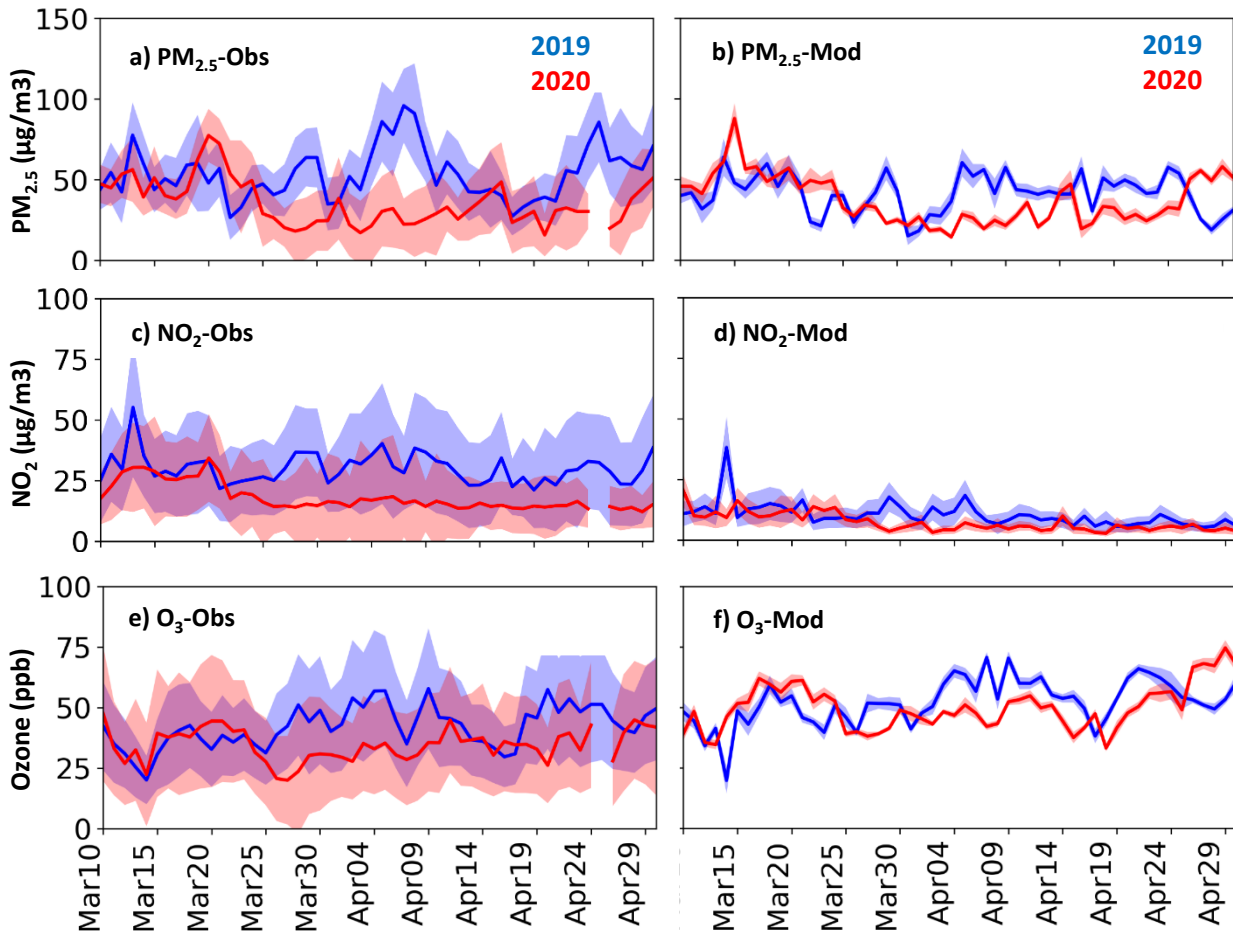
Figure S9 Averaged daytime (1000-1700 LT) PM$_{2.5}$ (top row), NO$_2$ (middle row), and ozone (bottom row) concentrations measured over CPCB stations in Delhi (left column) and modeled over Urban region (right column) between 10 March and 30 April in 2019 (green colors) and 2020 (red colors). The shaded regions show ±1STD. The observed data were extracted from the ground measurements data in Delhi, while the modeled data were averaged in the Urban box region.
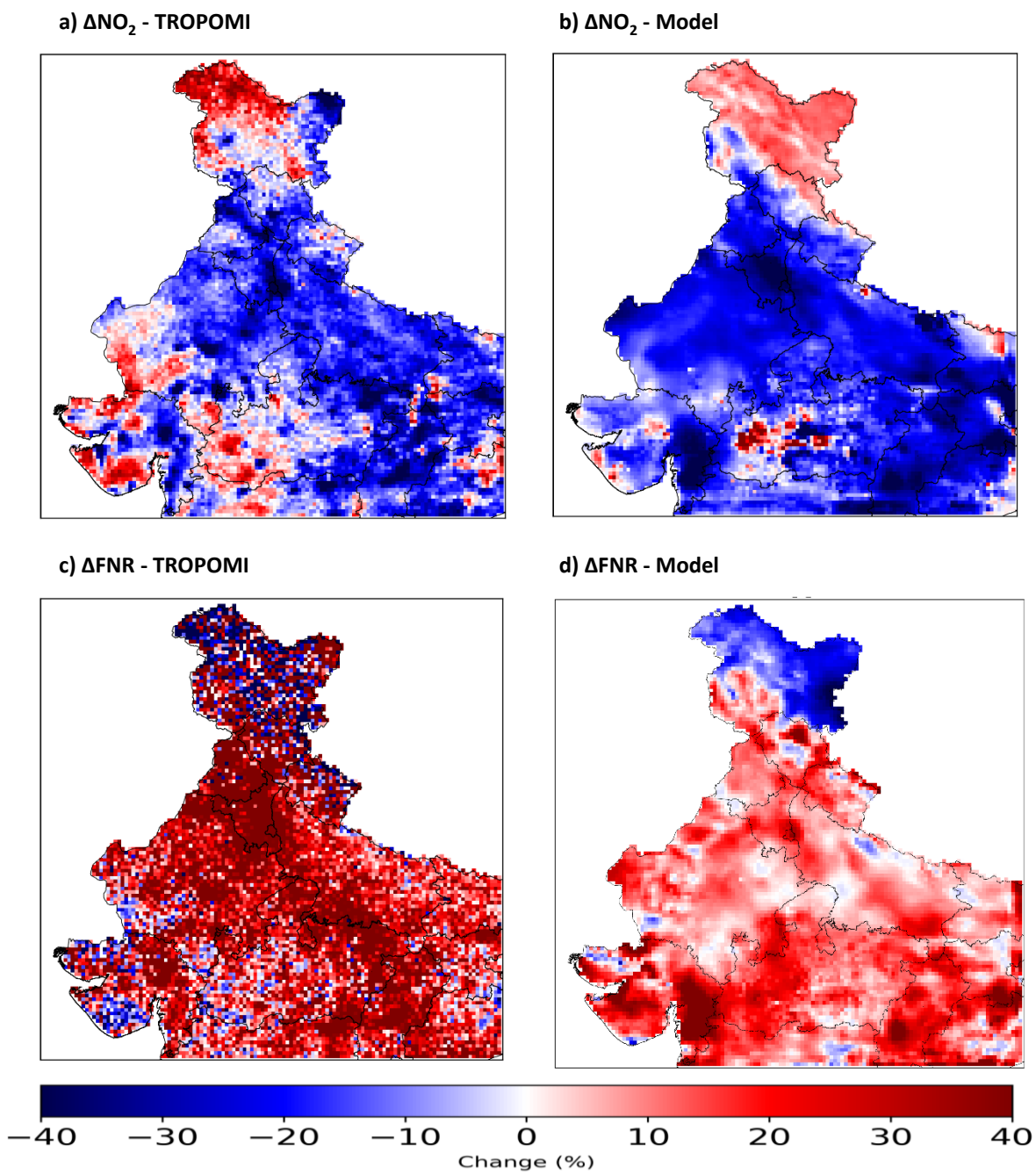
Figure S10 Changes in NO₂ tropospheric column (top row) and FNR (bottom row) between April 2020 and 2019 observed from the space (TROPOMI – left column) and modeled in this study (Model – right column). The modeled data are the mean values between 12:30 and 14:30 local time to resemble the TROPOMI overpass time.

a) Base

b) HTAP
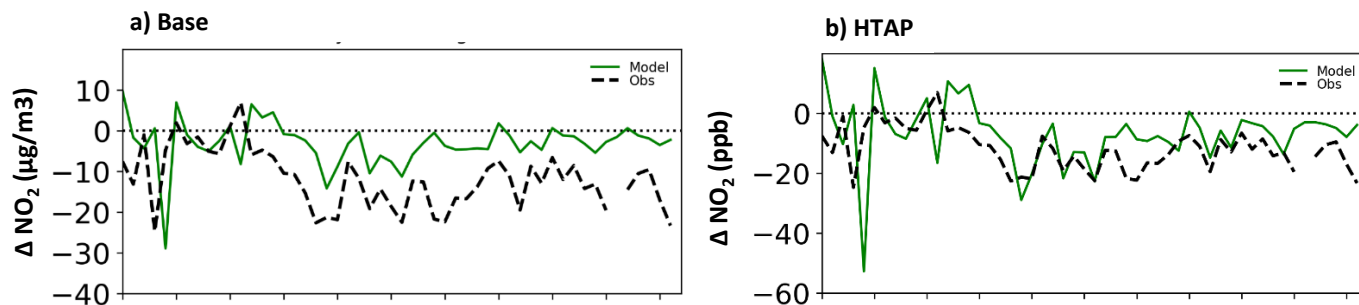
Figure S11 Averaged daytime (1000-1700 LT) NO₂ concentration changes between 2020 and 2019, during 10 March and 30 April, based on the measured data over CPCB stations in Delhi (black dashed line), Base model used in the manuscript, and using HTAP anthropogenic emission inventory instead of CEDS_M in the base model over Urban region. The observed data were extracted from the ground measurements data in Delhi, while the modeled data were averaged in the Urban box region
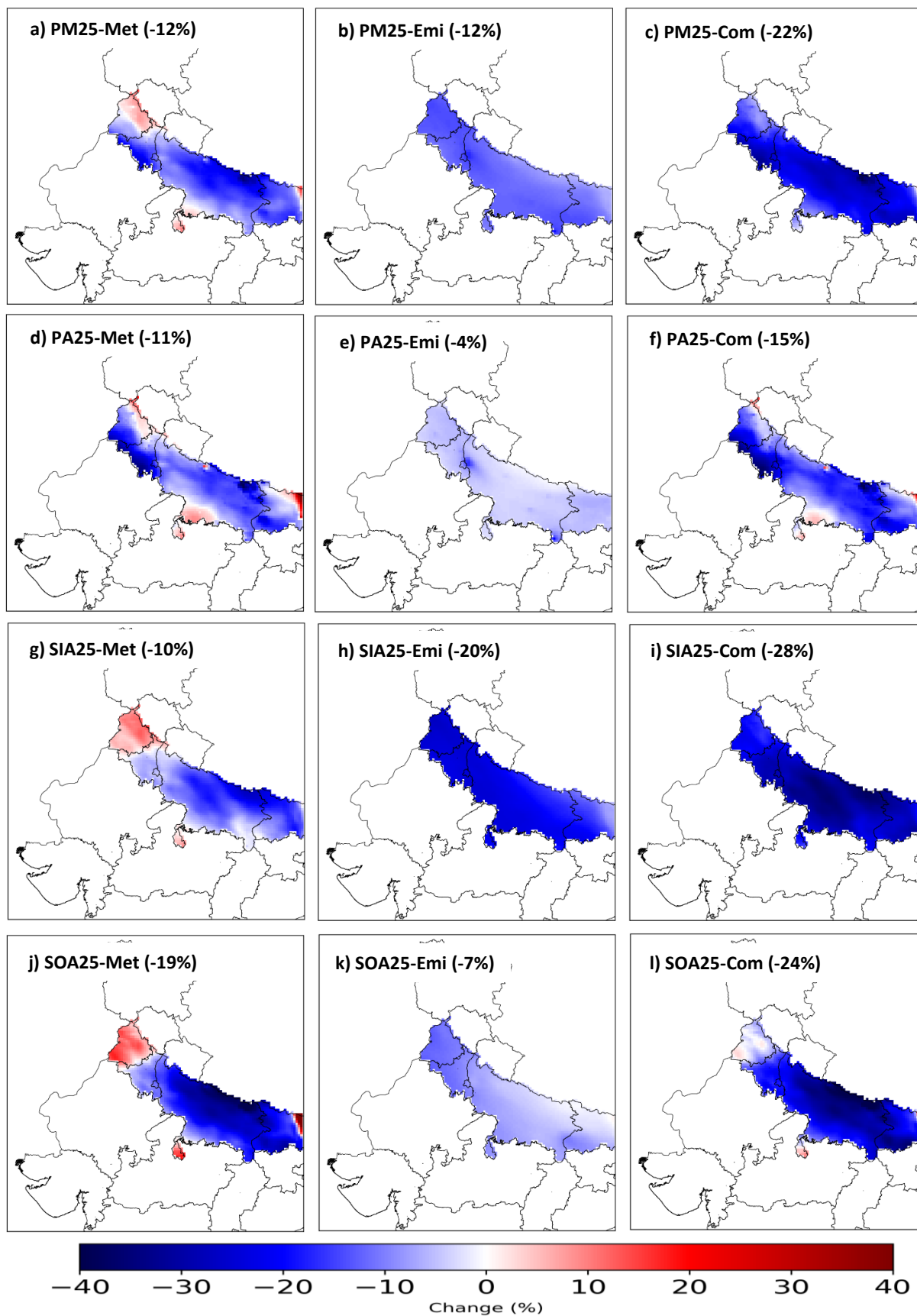
Figure S12 Responses of April averaged daytime PM$_{2.5}$ (first row), PA$_{2.5}$ (second row), SIA$_{2.5}$ (third row), and SOA$_{2.5}$ (fourth row) concentrations in the IGP to meteorology (left column), emission (middle column), and combined (right column) effects. The numbers in the parenthesis show the averaged change over the colored region between April 2020 and 2019.
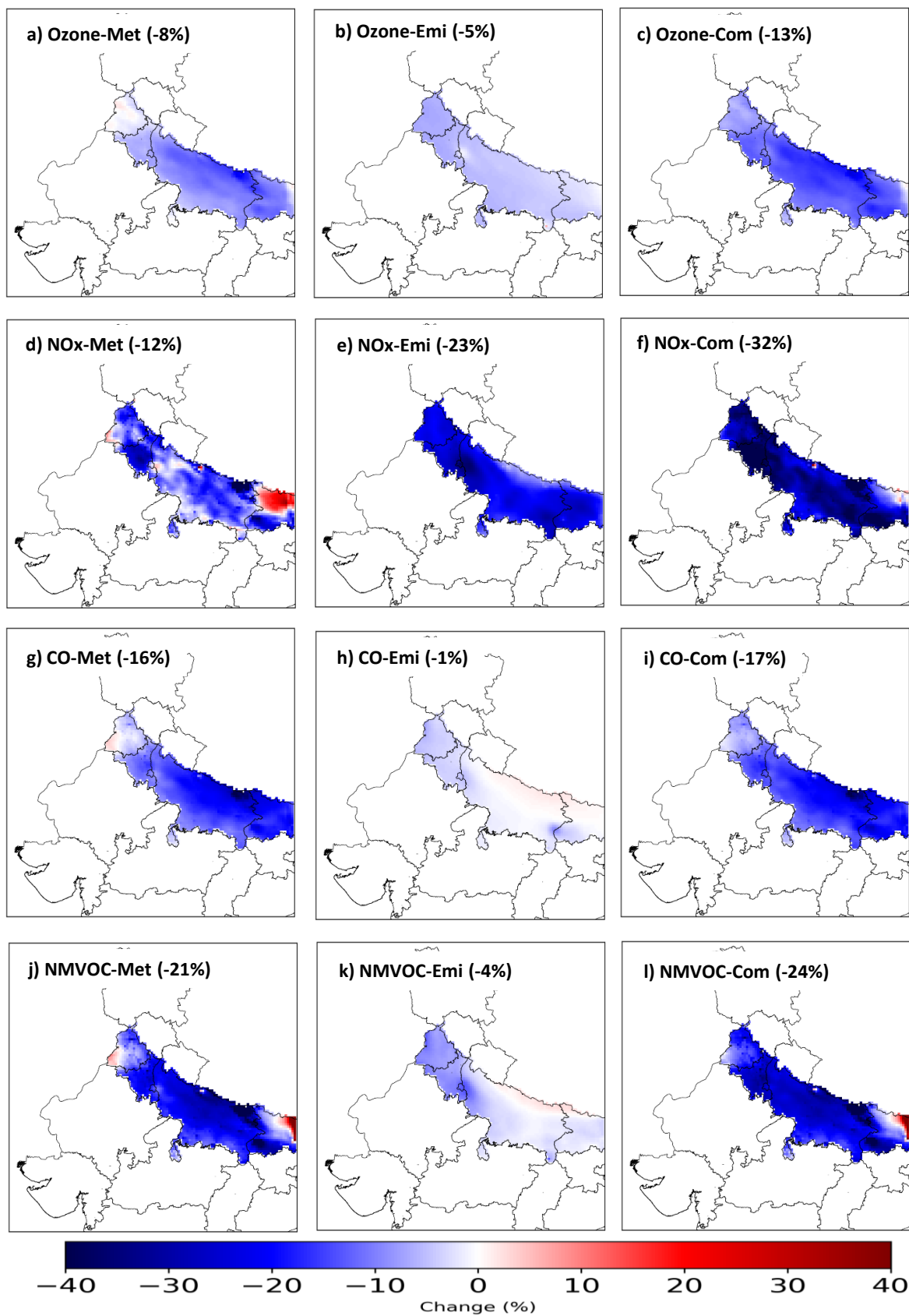
Figure S13 Responses of April averaged daytime ozone (first row), NOx (second row), CO (third row), and NMVOC (fourth row) concentrations in the IGP to meteorology (left column), emission (middle column), and combined (right column) effects. The numbers in the parenthesis show the averaged change over the colored region between April 2020 and 2019.
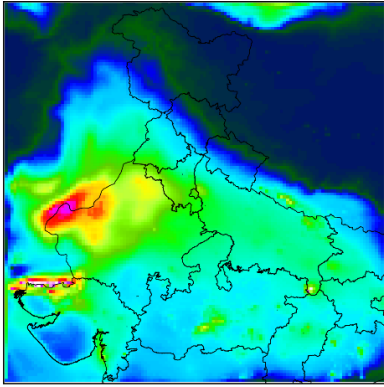
a) PA25-2019BAU **a) SIA25-2019BAU** **c) SOA25-2019BAU**
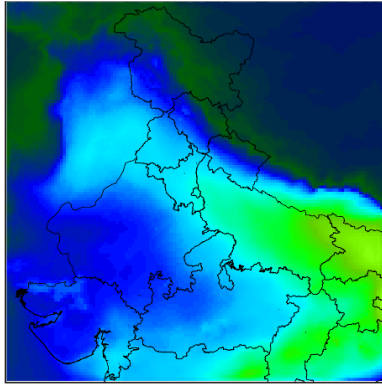
Concentration (μg/m3)
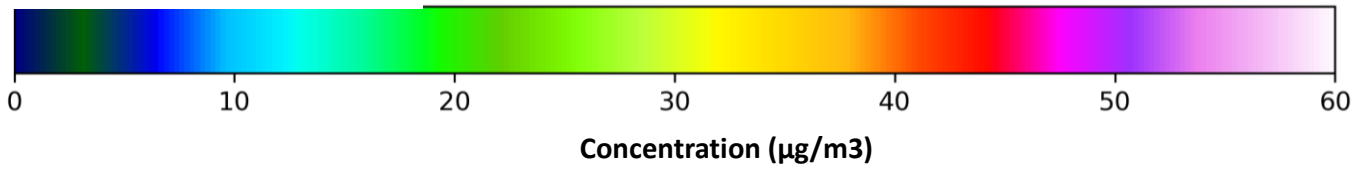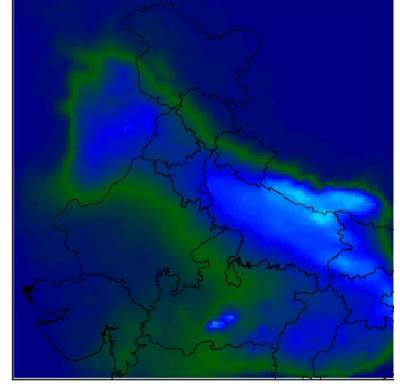
Figure S14 PM$_{2.5}$ composition concentrations averaged in April 2019 based on 2019BAU scenario
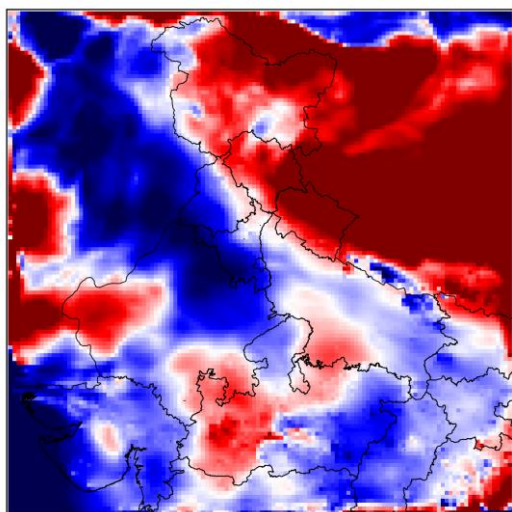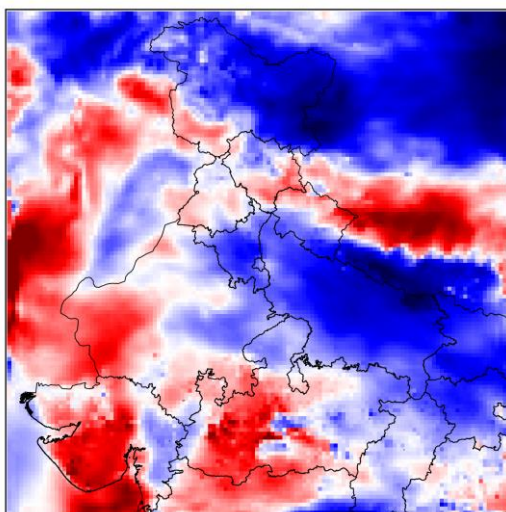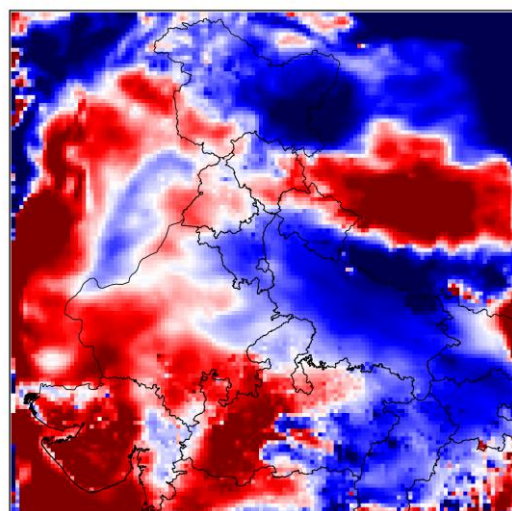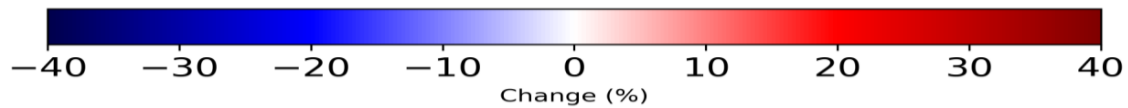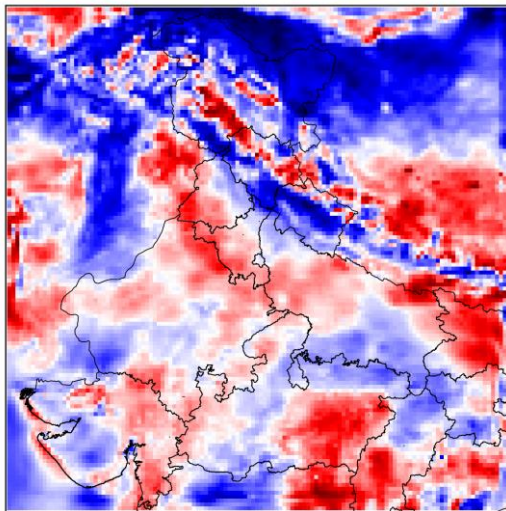
Figure S15 Responses of April averaged daytime a) primary inorganics (OIN$_{2.5}$), b) OC$_{2.5}$, c) BC$_{2.5}$, and d) 10-m wind speed (Ws10) to meteorology effects.
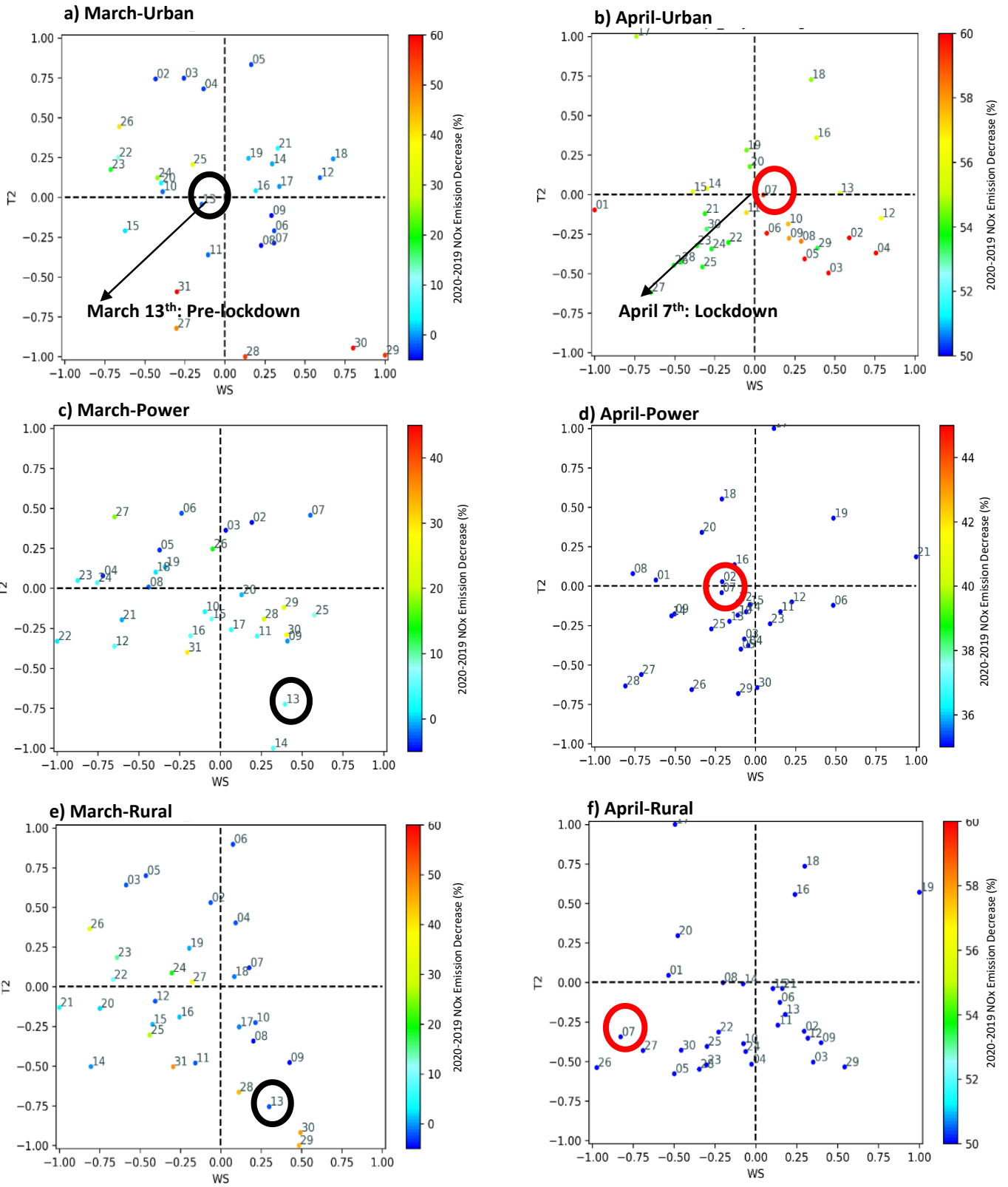
Figure S16 The changes between 2020 and 2019 in averaged daytime 2-m temperature (Y-axis) and 10-m wind speed (X-axis) in March (left column) and April (right column) in Urban (top row), Power (middle row), and Rural (bottom row). The numbers show the day of the month. The colors show the percentage of decrease in NOx emission in each day (negative value shows an increase in emission). The black (red) circle in top panel shows the day with the lowest overall changes in meteorology in March (April). X- and Y-axis are normalized changes.
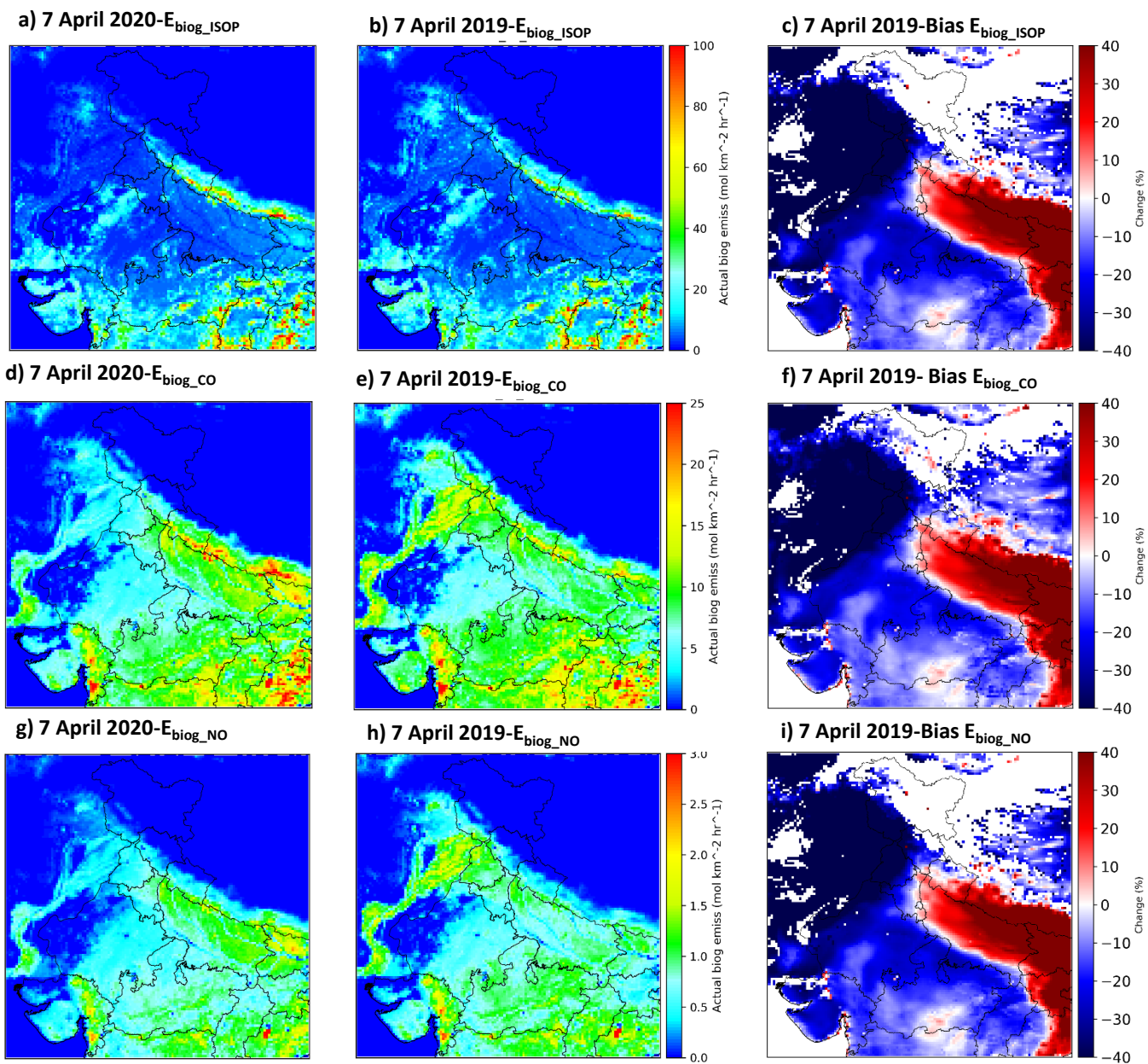
Figure S17 Biogenic emission from MEGAN in 7 April 2020 (left column) and 2019 (middle column) and their corresponding changes (right column) for isoprene (top row), CO (middle row), and NO (bottom row)

Absolute change [ug/m³ (left column), ppb (right column)]
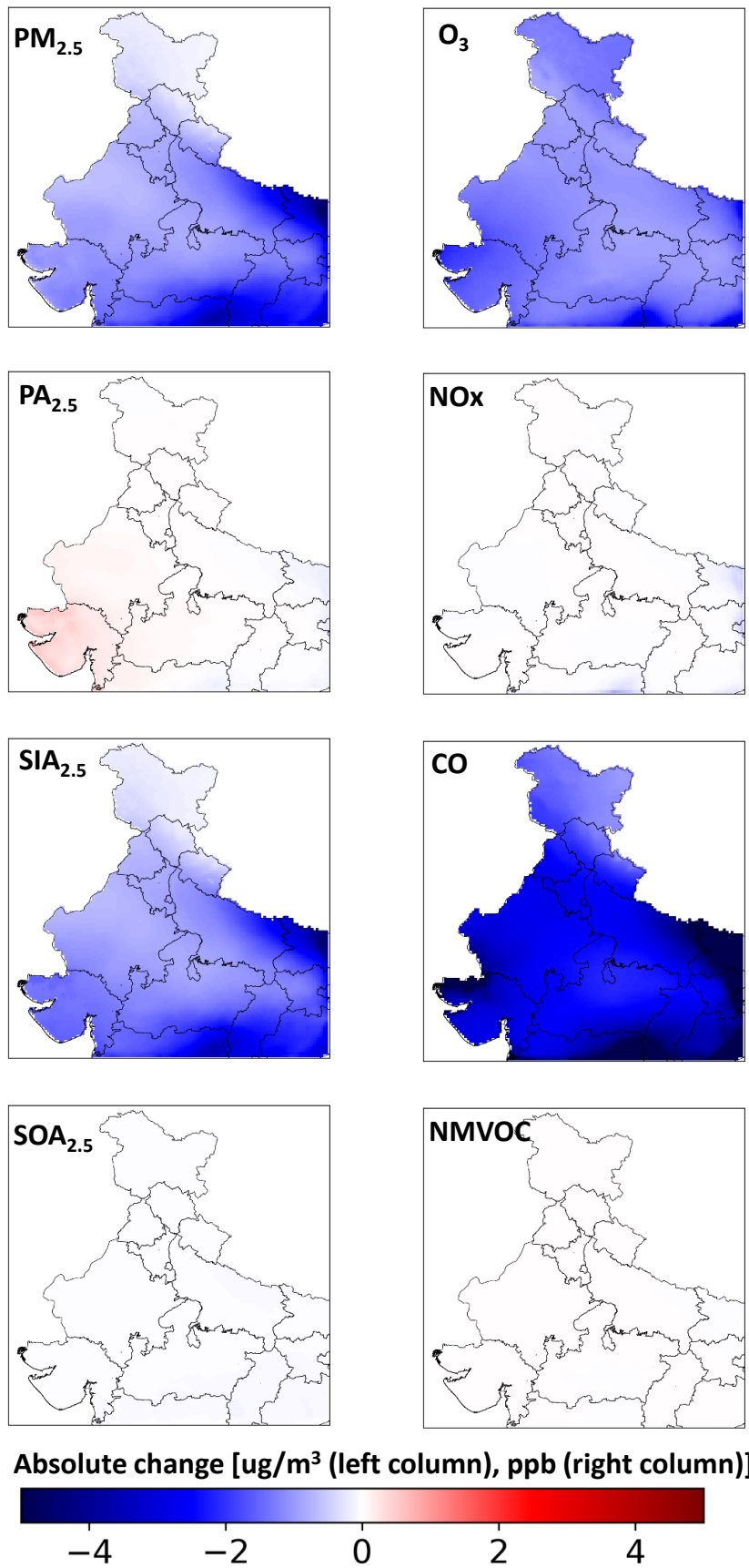
Figure S18 Impact of transboundary conditions due to the COVID-19 lockdown (COVID_BoundaryCondition – BAU_BoundaryCondition) over the domain on surface air pollutants concentrations
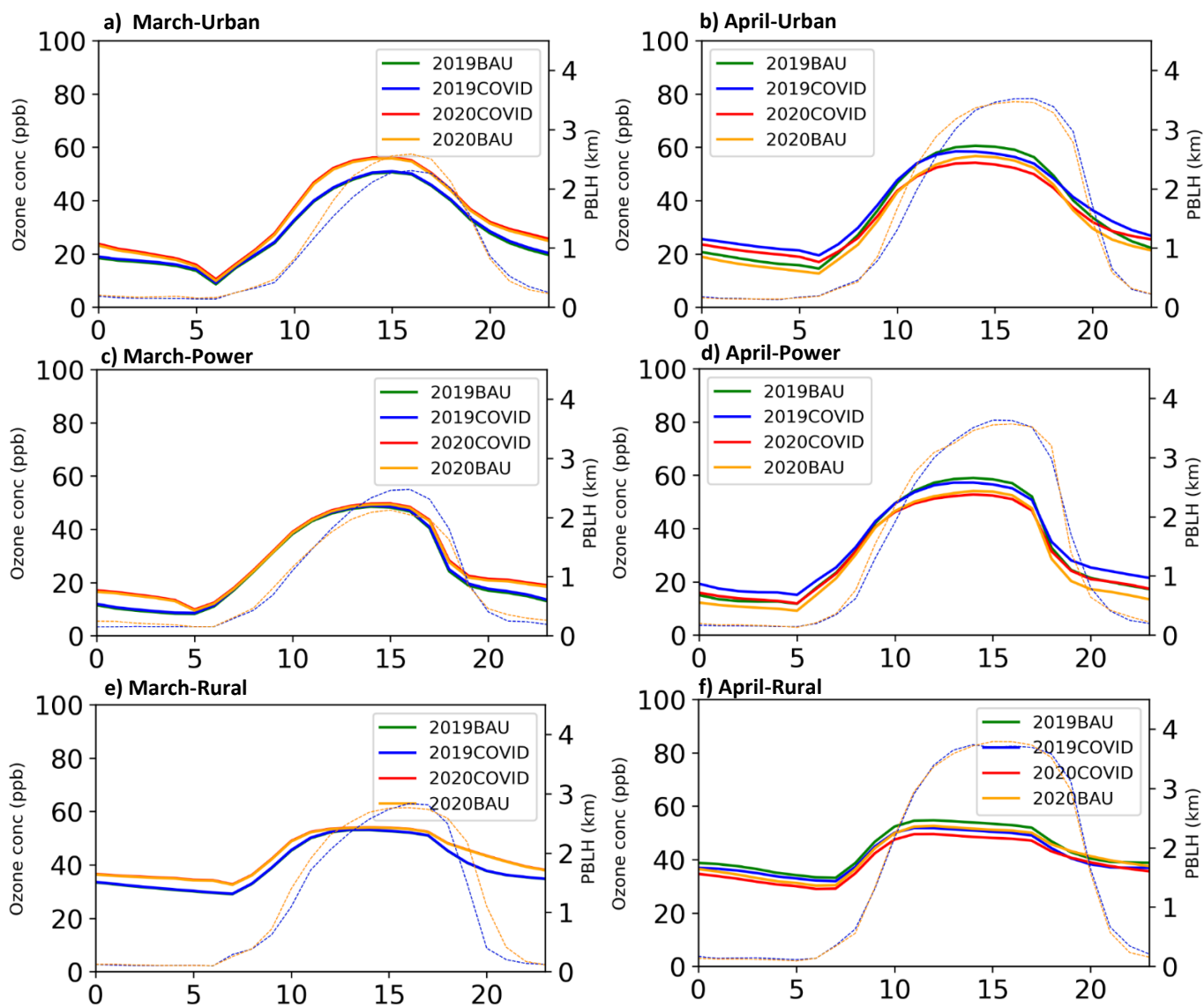
Figure S19 Surface ozone mixing ratio (primary Y-axis) and PBLH (secondary Y-axis) averaged over Urban (top row), Power (middle row), and Rural (bottom row) for a pre-lockdown days (10-24 March: left column) and lockdown days (1-31 April: right column). In each sub-plot, ozone concentration is shown with solid line and PBLH is shown with dotted line (blue for 2019, red for 2020). The results are shown for all the scenarios: 2019BAU (green), 2019COVID (blue), 2020BAU (orange), and 2020COVID (red).
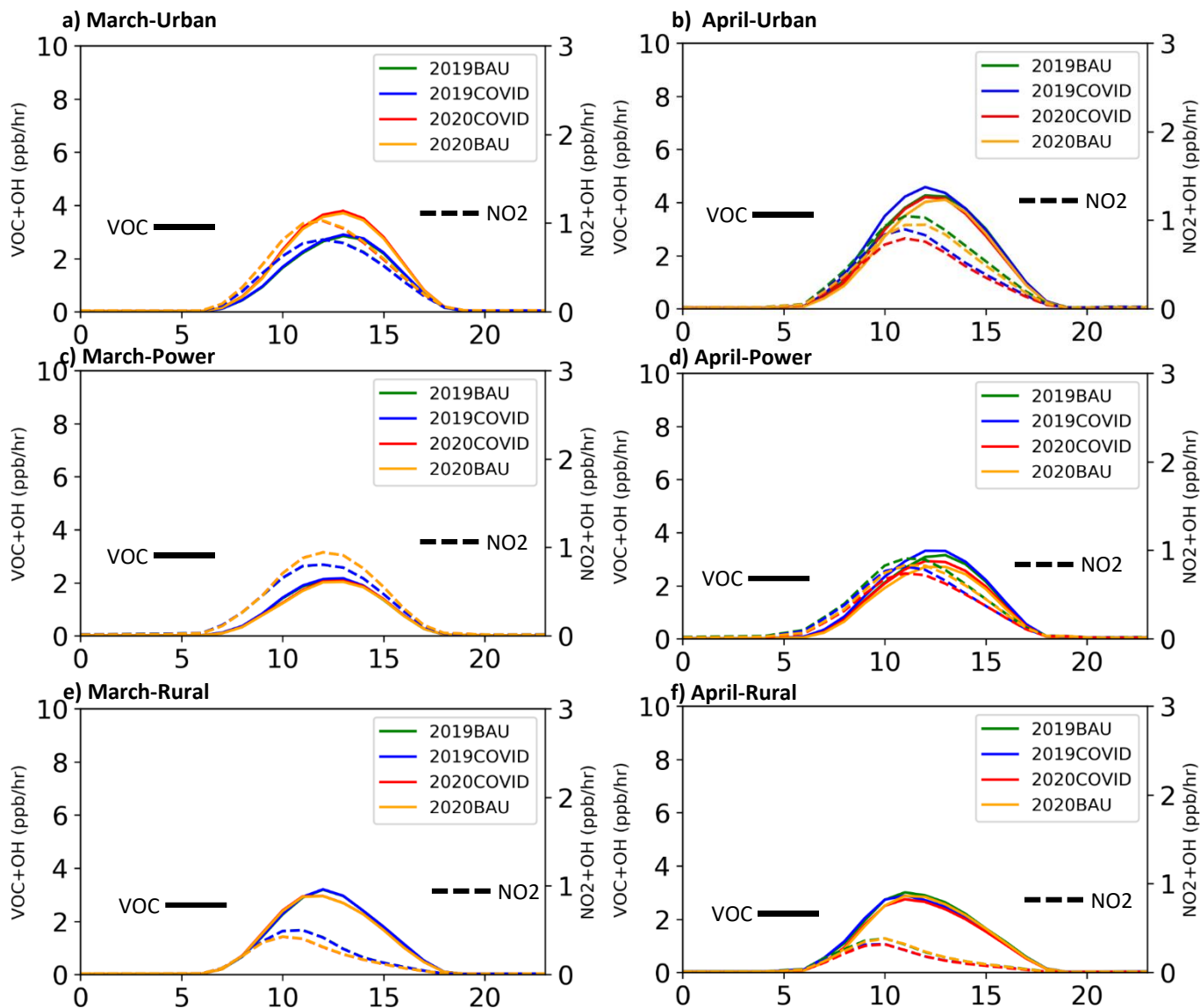
Figure S20 OH reactivity with VOCs (primary Y-axis) and NO$_2$ (secondary Y-axis) averaged within PBL over Urban (top row), Power (middle row), and Rural (bottom row) for pre-lockdown days (10-24 March: left column) and lockdown days (1-31 April: right column). In each sub-plot, OH reactivity with VOCs and NO$_2$ is shown with solid and dashed lines, respectively. The results are shown for all the scenarios: 2019BAU (green), 2019COVID (blue), 2020BAU (orange), and 2020COVID (red).
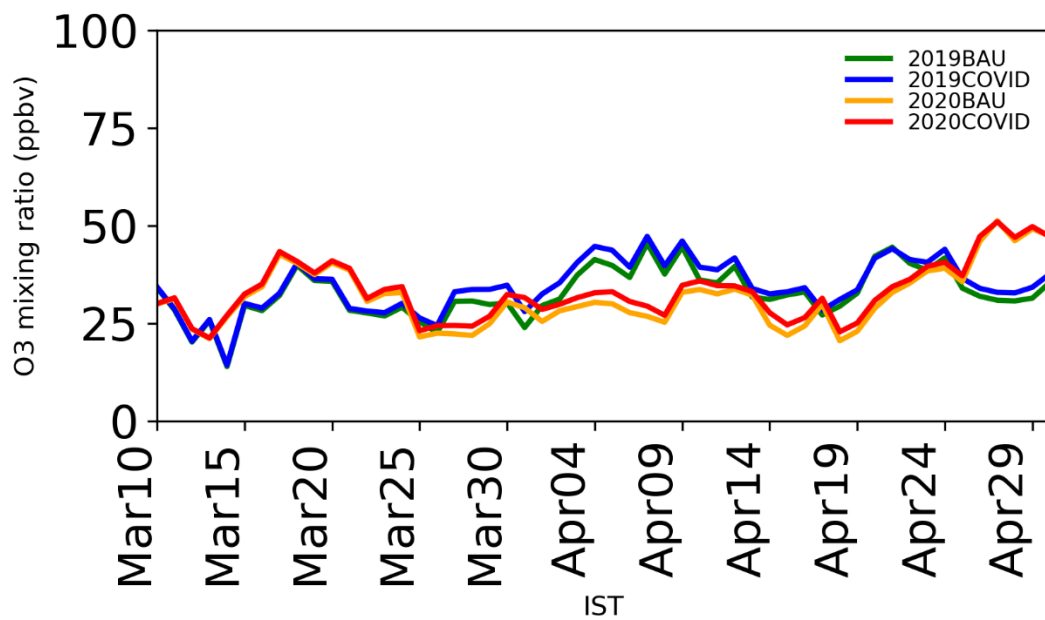
Figure S21 Daytime averaged ozone mixing ratio averaged within Urban region using all the scenarios
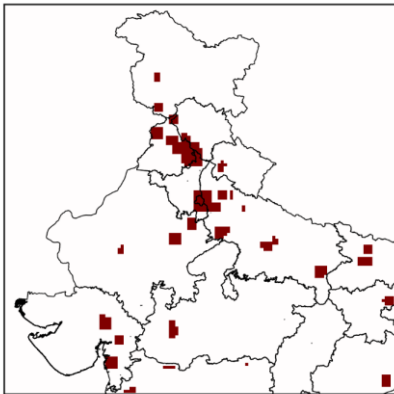
Figure S22 Grid cell classification based on NCAP cities and CEDS_M emission data. a) urban grid cells contain 32,580 grid cells, b) rural grid cells contain 734,130 grid cells, and c) power plant grid cells contain 28,800 grid cells.
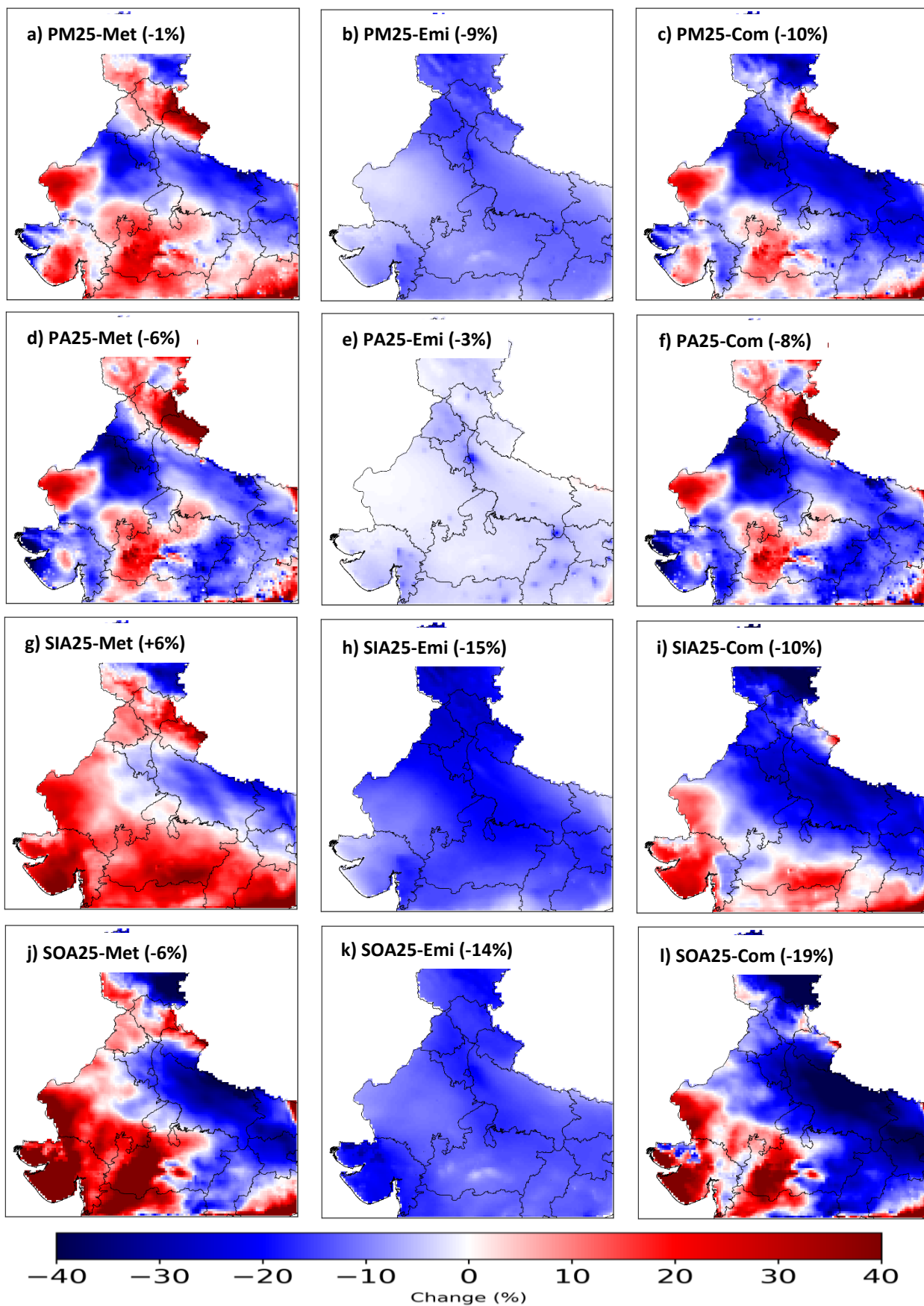
Figure S23 Same as Figure 7 in the main text using HTAP v2.2 anthropogenic emission inventory
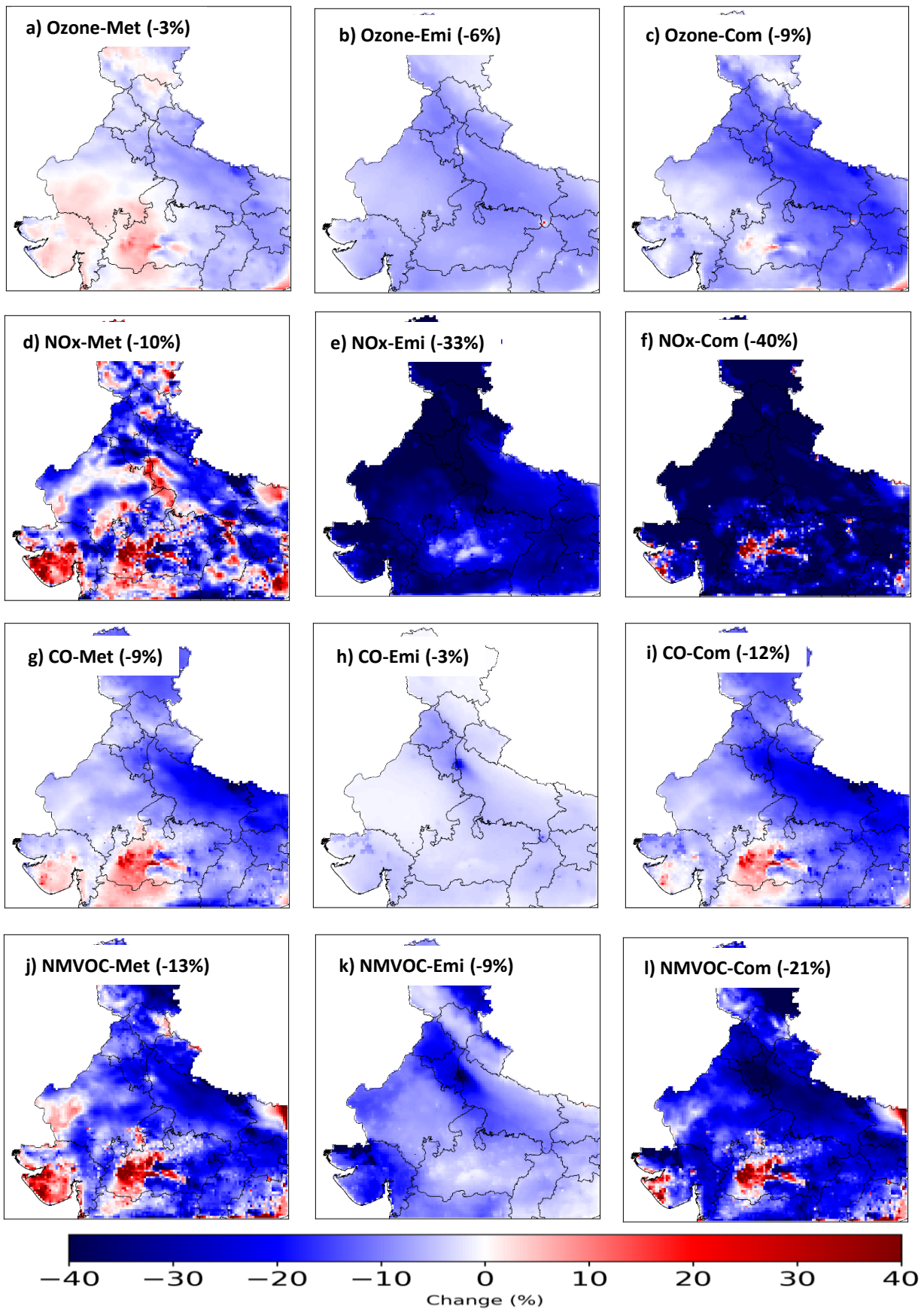
Figure S24 Same as Figure 8 in the main text using HTAP v2.2 anthropogenic emission inventory
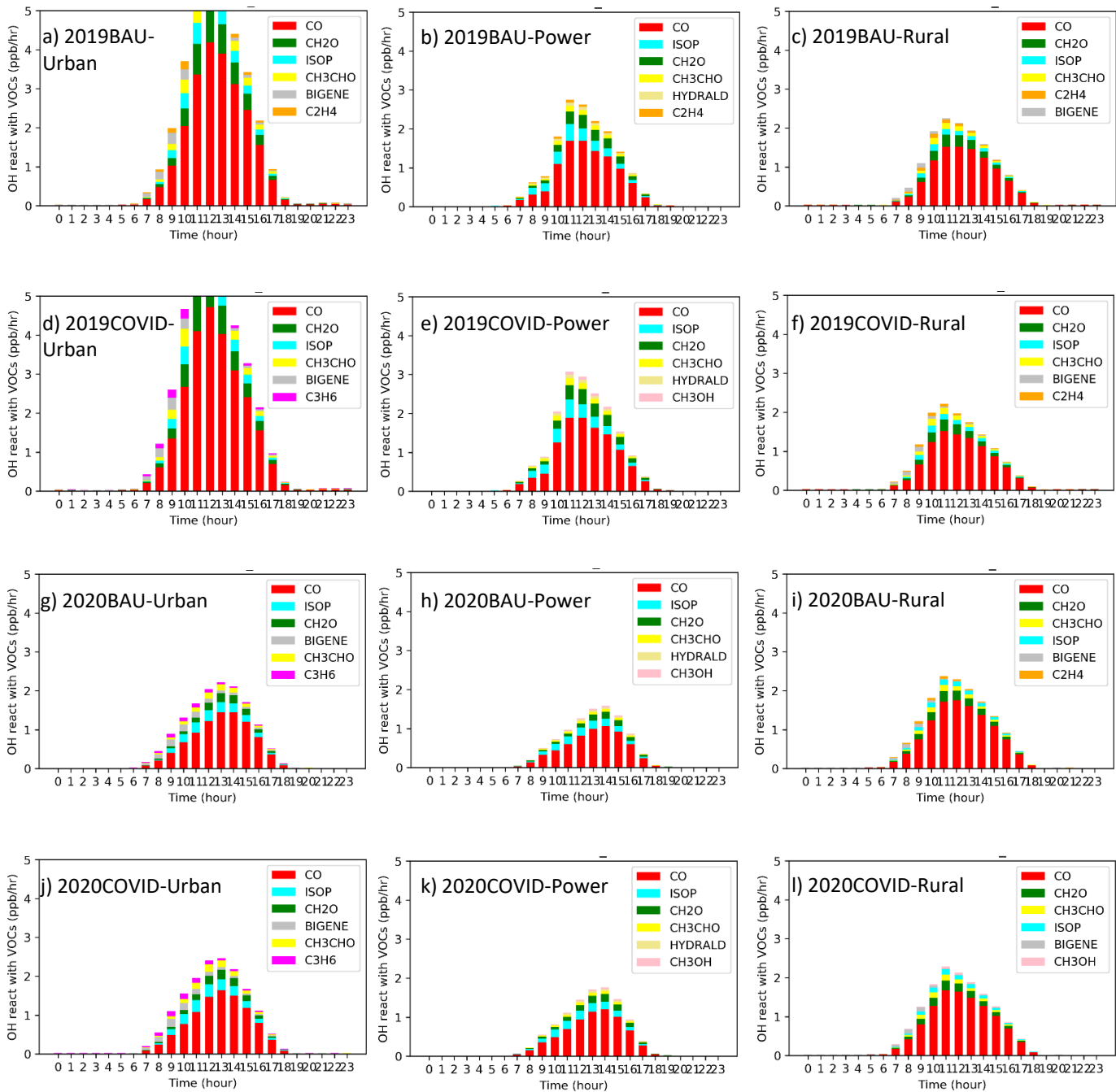
Figure S25 Diurnal cycle of OH reactivity with VOC species (averaged within the PBL) in Urban (left column), Power (middle column), and Rural (right column) for each scenario based on CEDS_M emission inventory. Only the first six VOC species with higher total contribution is shown. The legend in each panel shows the ranking of the species for each scenario.
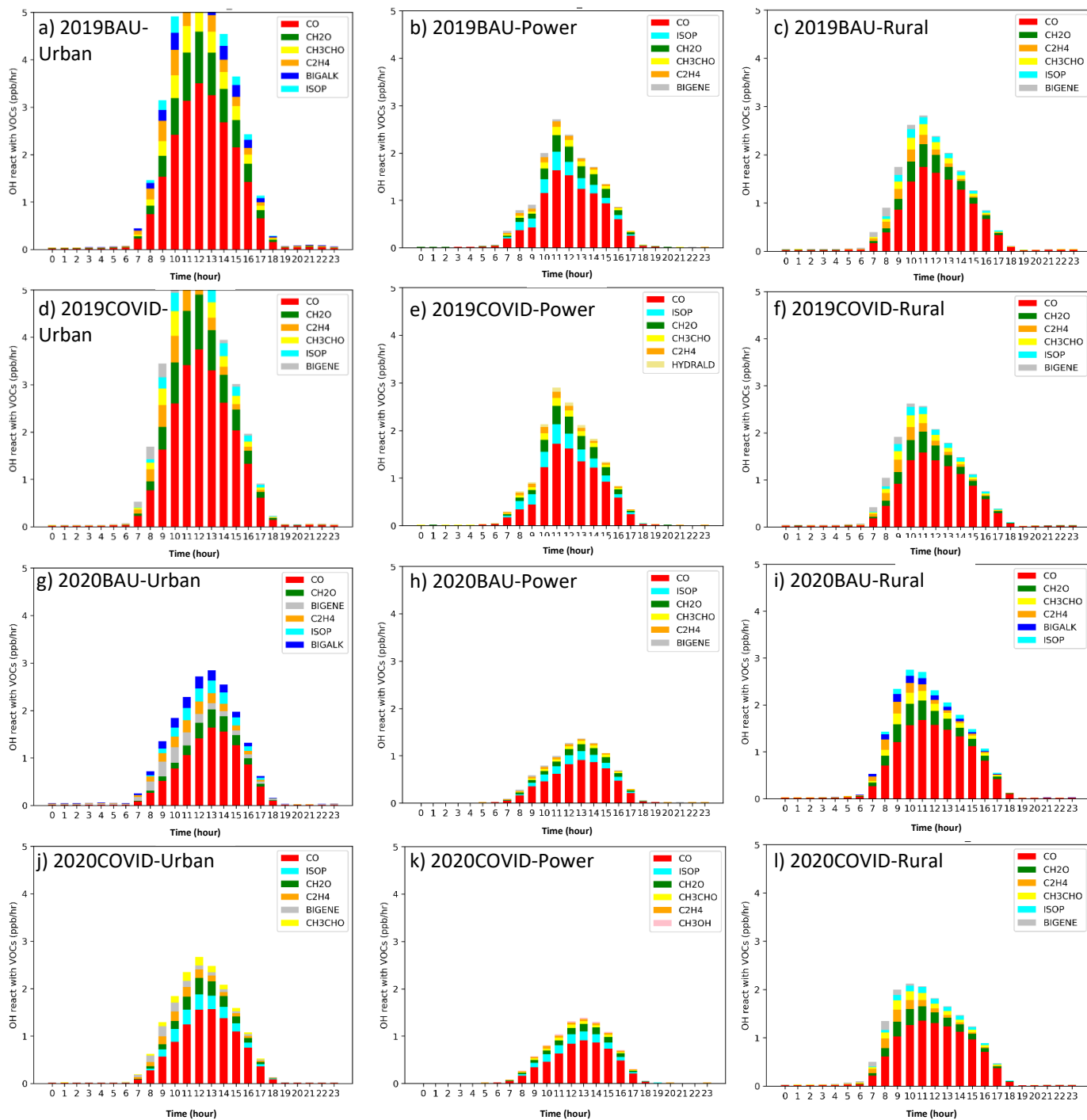
Figure S26 Same as Figure S24 using HTAP v2.2 emission inventory
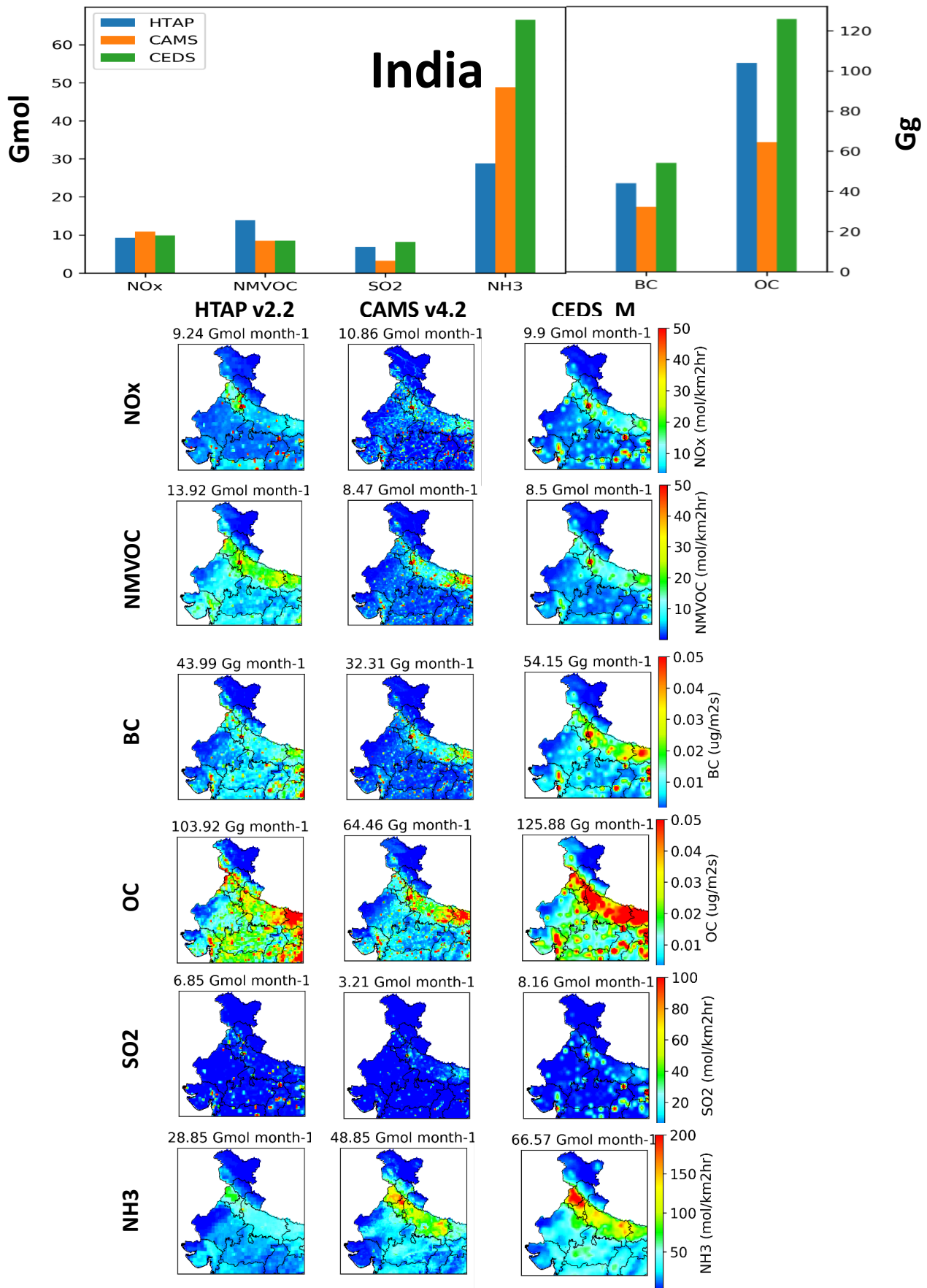
Figure S27 Comparison between HTAP v2.2, CAMS v4.2, and CEDS_M emission inventories
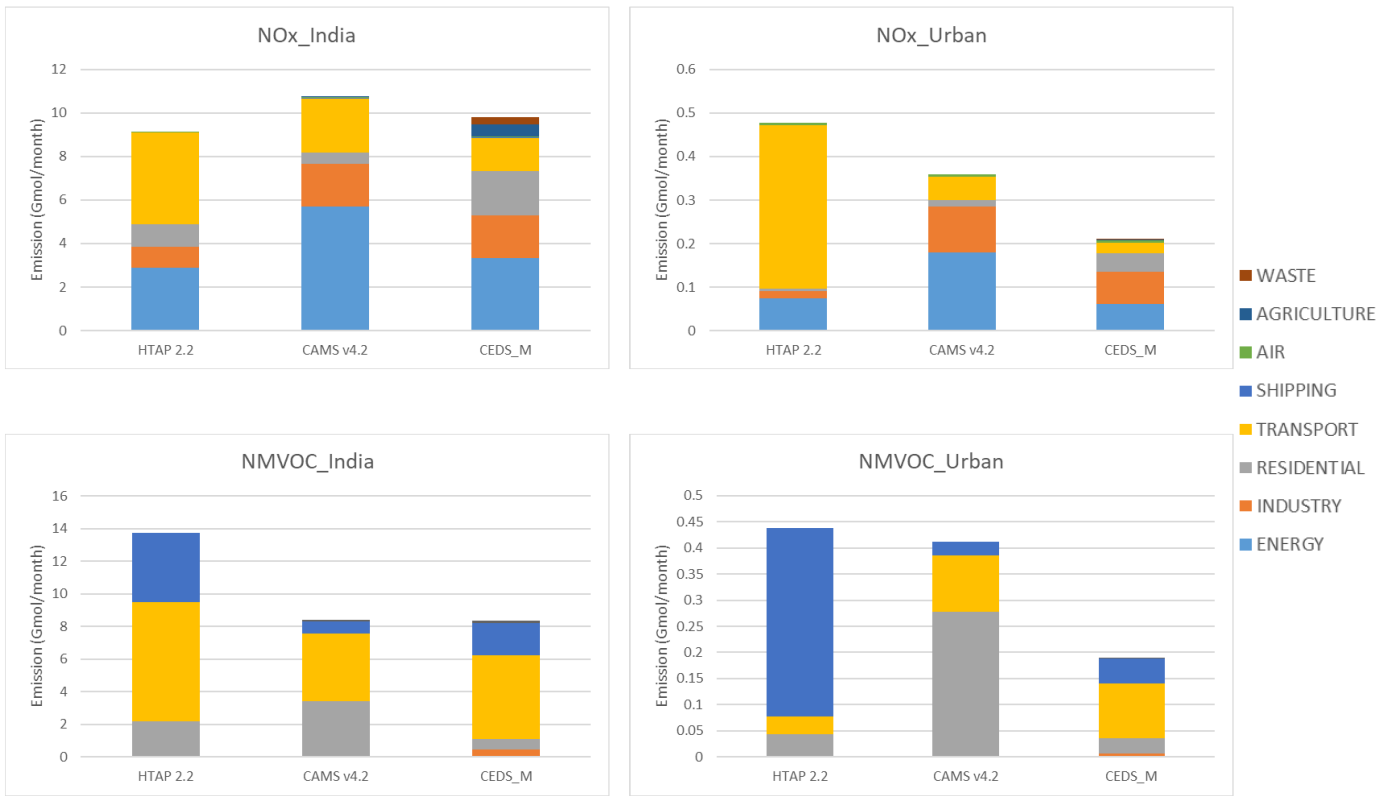
Figure S28 Sectoral Contribution in each emission inventory

Vertical Cross Section of O3 (ppb)
2019-03-04_06
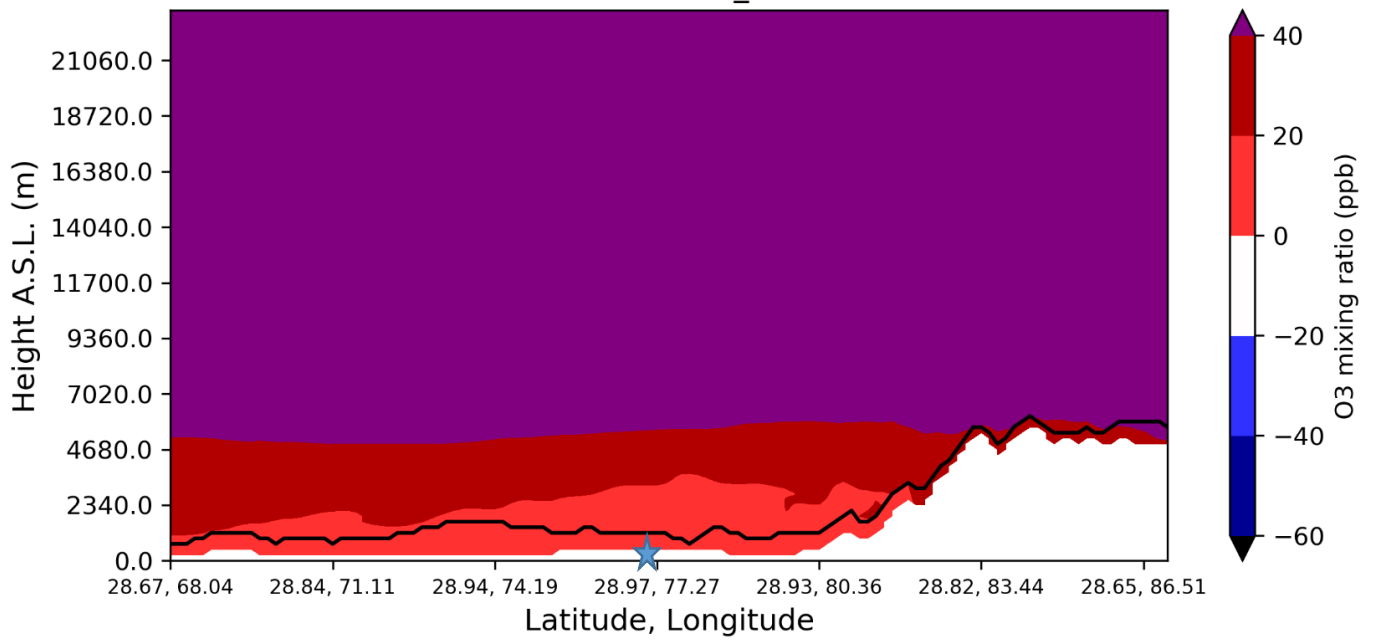
Figure S29 Cross section of ozone over India due to 50 percent more ozone in boundary conditions after 60 hours. The solid line shows the boundary layer height at each location. Star shows the approximate location of Delhi.

Table S1 The mapping between HTAP v2.2 and CAMS v4.2 VOC species to MOZART mechanism in WRF-Chem

MOZART	HTAP	CAMS
C2H2	ethyne	voc9
C2H4	ethene	voc7
C2H6	ethane	voc2
C3H6	propene	voc8
C3H8	propane	voc3
BIGALK	butanes + pentanes + hexanes&higher-alkanes + esters + ethers	voc4+voc5+voc6+voc18+voc19
BIGENE	other-alkenes	voc12
BENZENE	benzene	voc13
TOLUENE	toluene	voc14
XYLENES	xylene + trimethylbenzenes + other-aromatics	voc15+voc16+voc17
CH2O	methanal	voc21
CH3CHO	other-alkanals (aldehydes)	voc22
CH3OH	0.15 * alcohols	0.15*voc1
C2H5OH	0.85 * alcohols	0.85*voc1
CH3COCH3	0.2 * ketones	0.2*voc23
MEK	0.8 * ketones	0.8*voc23
HCOOH	0.5 * acids	0.5*voc24
CH3COOH	0.5 * acids	0.5*voc24
ISOP		voc10
C10H16		voc11

Table S2 Total emissions in CEDS_M inventory using BAU and COVID scenarios in March

Species (unit)	India		Urban		Power		Rural	
	BAU	COVID	BAU	COVID	BAU	COVID	BAU	COVID
NMVOC (Gmol)	8.83	8.77	0.19	0.19	0.04	0.04	0.01	0.01
NOx (Gmol)	10.23	9.69	0.22	0.20	0.28	0.27	0.01	0.01
CO (Gmol)	114.92	113.89	2.20	2.17	0.27	0.26	0.17	0.17
SO$_2$ (Gmol)	8.44	7.74	0.19	0.17	0.34	0.33	0.00	0.00
BC (Gg)	56.18	55.34	1.40	1.34	0.42	0.40	0.08	0.08
OC (Gg)	130.76	132.59	2.80	2.78	1.64	1.58	0.22	0.23

Table S3 Total emissions in CEDS_M inventory using BAU and COVID scenarios in April

Species (unit)	India		Urban		Power		Rural	
	BAU	COVID	BAU	COVID	BAU	COVID	BAU	COVID
NMVOC (Gmol)	8.50	8.01	0.19	0.16	0.04	0.03	0.01	0.01
NOx (Gmol)	9.90	7.36	0.21	0.14	0.27	0.21	0.01	0.01
CO (Gmol)	110.69	103.23	2.13	1.93	0.26	0.22	0.17	0.18
SO$_2$ (Gmol)	8.16	4.97	0.19	0.10	0.33	0.25	0.00	0.00
BC (Gg)	54.15	49.08	1.35	1.07	0.40	0.32	0.08	0.09
OC (Gg)	125.88	130.23	2.7	2.5	1.6	1.3	0.21	0.24

Table S4 Total biogenic and biomass burning emissions in April 2019 and April 2020. The results are in Mega moles (Mmol) and Mega grams (Mg) for gaseous and aerosol species, respectively, in Urban, Power, and Rural regions. For India, the results are in Giga moles (Gmol) and Giga grams (Gg) for gaseous and aerosol species, respectively.

Biogenic emissions								
	India (Gmol or Gg)		Urban (Mmol or Mg)		Power (Mmol or Mg)		Rural (Mmol or Mg)	
Species (gas/aerosol)	2019	2020	2019	2020	2019	2020	2019	2020
NMVOC (gas)	8.03	7.64	14.49	13.66	15.04	14.22	6.50	6.14
NOx (gas)	0.61	0.53	1.55	1.29	1.35	1.16	1.53	1.26
CO (gas)	5.82	5.25	13.16	11.28	13.00	11.48	11.82	10.23
Biomass Burning Emission								
	India (Gmol or Gg)		Urban (Mmol or Mg)		Power (Mmol or Mg)		Rural (Mmol or Mg)	
Species (gas/aerosol)	2019	2020	2019	2020	2019	2020	2019	2020
NMVOC (gas)	12.31	10.10	4.12	0.82	8.07	0.23	10.04	4.13
NOx (gas)	1.68	1.37	0.54	0.19	1.25	0.05	1.31	0.54
CO (gas)	52.25	42.11	16.72	3.88	34.79	1.06	40.77	16.79
SO_2 (gas)	0.13	0.1	0.03	0.02	0.11	0.00	0.08	0.03
BC (aerosol)	8.15	6.60	2.62	0.62	5.25	0.17	6.40	2.63
OC (aerosol)	52.64	38.78	13.69	3.93	35.95	1.03	33.38	13.75

Table S5 Table of statistics including Mean (± standard deviation), Normalized Mean Bias (NMB), Root Mean Square Error (RMSE), and Pearson Correlation Coefficient averaged for all CPCB stations in Delhi in April 2019 (scenario: 2019BAU) and 2020 (scenario: 2020COVID) using CEDS_M anthropogenic emission inventories. 17285 and 22880 hourly points prior to applying filters were used in 2019 and 2020, respectively.

Variable	Year	OBS Mean (±1std)	MODEL Mean (±1std)	NMB (%)	RMSE	R (%)
O₃ MDA8 (ppb)	2019	47(±7)	55(±7)	+18	11	+39
	2020	33(±5)	45(±8)	+36	14	+48
PM₂.₅ 24 hours (µg/m3)	2019	82(±40)	68(±27)	-17	35	+59
	2020	45(±23)	50(±21)	+11	20	+61
PM₂.₅ daytime (µg/m3)	2019	56(±22)	43(±14)	-24	24	+45
	2020	30(±13)	32(±13)	+7	14	+47
NO₂ 24 hours (µg/m3)	2019	46(±20)	39(±26)	-15	23	+58
	2020	20(±7)	27(±19)	+38	17	+59

The column header "CEDS_M" spans the MODEL Mean, NMB, RMSE, and R columns.

Table S6 Statistics for air quality predictions in April 2019 using three scenarios. HTAP refers to using HTAP v2.2 as anthropogenic emission inventory. CEDS_M refers to use of CEDS_M emission inventory. CEDS_0.75NOXnight_1.25NOXday_0.5BC refers to using CEDS_M with a simple diurnal profile on NOx and half ozone from boundary condition (base scenario in the main text).

Variable	OBS Mean (±1std)	HTAP				CEDS_M				CEDS_0.75NOXnight_1.25NOXday_0.5BC			
		MODEL Mean (±1std)	NMB (%)	RMSE	R (%)	MODEL Mean (±1std)	NMB (%)	RMSE	R (%)	MODEL Mean (±1std)	NMB (%)	RMSE	R (%)
O$_3$ MDA8 (ppb)	47(±7)	68(±9)	+44	22	+64	71(±7)	+50	24	+54	55(±7)	+18	11	+39
PM$_{2.5}$ 24 hours (µg/m3)	82(±40)	56(±20)	-31	42	+53	69(±27)	-16	35	+59	68(±27)	-17	35	+59
NO$_2$ 24 hours (µg/m3)	46(±20)	70(±45)	+51	42	+68	46(±34)	0.24	28	+60	39(±26)	-15	23	+58

Table S7 Responses of averaged daytime air pollutant concentrations, in percentage, to changes in meteorology (2020BAU-2019BAU), COVID19 lockdown emissions (2020COVID-2020BAU), and combined effects (2020COVID-2019BAU) in different regions. The Urban, Rural, and Power regions are the predefined representative box regions. The numbers in the parenthesis show the minimum and maximum values.

Region	Species	Meteorology (min, max)	COVID-19 lockdown emission (min, max)	Combined (min, max)
India	$PM_{2.5}$	**-2%** (-36%, +110%)	**-9%** (-19%, 0%)	**-11%** (-40%, +90%)
	$PA_{2.5}$	**-6%** (-57%, +141%)	**-3%** (-20%, +0%)	**-9%** (-56%, +128%)
	$SIA_{2.5}$	**+5%** (-33% +80%)	**-16%** (-29%, +0%)	**-12%** (-45%, +69%)
	$SOA_{2.5}$	**-5%** (-51%, +5.4E3%)	**-8%** (-30%, +1%)	**-13%** (-60%, +5.2E3)
	O_3	**-3%** (-21%, +23%)	**-4%** (-9%, 6%)	**-8%** (-24%, +20%)
	NOx	**-9%** (-68%, 158%)	**-22%** (-57%, +0%)	**-30%** (-71%, +152%)
	CO	**-8%** (-43%, 50%)	**-2%** (-20%, +0%)	**-10%** (-42%, +50%)
	NMVOC	**-14%** (-66%, 192%)	**-3%** (-42%, +3%)	**-17%** (-65%, +191%)
IGP	$PM_{2.5}$	**-12%** (-35%, +22%)	**-12%** (-20%, -4%)	**-22%** (-40%, +14%)
	$PA_{2.5}$	**-11%** (-39%, +59%)	**-4%** (-20%, +0%)	**-15%** (-40%, +53%)
	$SIA_{2.5}$	**-10%** (-28%, 14%)	**-20%** (-27%, -6%)	**-28%** (-37%, +1%)
	$SOA_{2.5}$	**-19%** (-46%, +140%)	**-7%** (-13%, +1%)	**-24%** (-46%, +142%)
	O_3	**-8%** (-22%, +4%)	**-5%** (-7%, +6%)	**-13%** (-24%, +4%)
	NOx	**-12%** (-64%, 41%)	**-23%** (-39%, -4%)	**-32%** (-67%, +35%)
	CO	**-16%** (-43%, +4%)	**-1%** (-10%, +2%)	**-17%** (-42%, -1%)
	NMVOC	**-21%** (-66%, +158%)	**-4%** (-13%, +3%)	**-24%** (-65%, +148%)

Table S7 (Continued)

Region	Species	Meteorology (min, max)	COVID-19 lockdown emission (min, max)	Combined (min, max)
Urban	PM$_{2.5}$	**-11%** (-15%, -6%)	**-15%** (-17%, -13%)	**-25%** (-27%, -21%)
	PA$_{2.5}$	**-14%** (-24%, -6%)	**-11%** (-16%, -5%)	**-24%** (-28%, -18%)
	SIA$_{2.5}$	**-5%** (-6%, -3%)	**-24%** (-24%, -24%)	**-28%** (-29%, -27%)
	SOA$_{2.5}$	**-12%** (-16%, -9%)	**-8%** (-10%, -6%)	**-19%** (-21%, -18%)
	O$_3$	**-7%** (-9%, -6%)	**-3%** (-6%, -1%)	**-10%** (-12%, -9%)
	NOx	**-7%** (-26%, +5%)	**-35%** (-39%, -30%)	**-39%** (-49%, -33%)
	CO	**-10%** (-14%, -8%)	**-4%** (-5%, -4%)	**-14%** (-17%, -12%)
	NMVOC	**-16%** (-24%, -11%)	**-12%** (-13%, -10%)	**-26%** (-32%, -22%)
Rural	PM$_{2.5}$	**+2%** (-0%, +4%)	**-12%** (-12%, -12%)	**-10%** (-12%, -8%)
	PA$_{2.5}$	**+8%** (+5%, +9%)	**-4%** (-4%, -3%)	**+4%** (+0%, +6%)
	SIA$_{2.5}$	**-1%** (-5%, +2%)	**-24%** (-24%, -24%)	**-25%** (-28%, -22%)
	SOA$_{2.5}$	**-4%** (-8%, +2%)	**-8%** (-8%, -8%)	**-12%** (-16%, -7%)
	O$_3$	**-4%** (-6%, -2%)	**-6%** (-6%, -5%)	**-10%** (-11%, -8%)
	NOx	**-6%** (-13%, -2%)	**-17%** (-19%, -16%)	**-22%** (-29%, -18%)
	CO	**-9%** (-10%, -7%)	**-1%** (-1%, -1%)	**-10%** (-12, -8%)
	NMVOC	**-15%** (-22%, -11%)	**-3%** (-3%, -2%)	**-17%** (-24%, -12%)
Power	PM$_{2.5}$	**-7%** (-10%, -3%)	**-16%** (-19%, -14%)	**-21%** (-24%, -18%)
	PA$_{2.5}$	**-8%** (-14%, -3%)	**-14%** (-20%, -8%)	**-21%** (-26%, -13%)
	SIA$_{2.5}$	**-1%** (-3%, +2%)	**-20%** (-21%, -18%)	**-21%** (-22%, -19%)
	SOA$_{2.5}$	**-18%** (-20%, -15%)	**-7%** (-8%, -6%)	**-24%** (-25%, -22%)
	O$_3$	**-8%** (-9%, -6%)	**-2%** (-4%, +6%)	**-10%** (-12%, -3%)
	NOx	**-5%** (-20%, +4%)	**-26%** (-28%, -25%)	**-30%** (-41%, -23%)
	CO	**-12%** (-13%, -12%)	**-2%** (-4%, -2%)	**-14%** (-15%, -13%)
	NMVOC	**-17%** (-22%, -13%)	**-6%** (-12%, -4%)	**-22%** (-26%, -20%)

Table S8 Reactions used to calculate the LROx in IRR analysis

MOZART Reactions	IRR reactions (LROx)
ALKO2 + HO2 -> ALKOOH	ALKO2_HO2_IRR
BENZO2 + HO2 -> BENZOOH	BENZO2_HO2_IRR
BZOO + HO2 -> BZOOH	BZOO_HO2_IRR
C2H5O2 + HO2 -> C2H5OOH + O2	C2H5O2_HO2_IRR
C3H7O2 + HO2 -> C3H7OOH + O2	C3H7O2_HO2_IRR
C6H5O2 + HO2 -> C6H5OOH	C6H5O2_HO2_IRR
CH3O2 + HO2 -> CH3OOH + O2	CH3O2_HO2_IRR
HO2 + HO2 -> H2O2 + O2	HO2_HO2_H2O_IRR
HO2 + aer -> 0.5*H2O2	HO2_IRR
HOCH2OO + HO2 -> HCOOH	HOCH2OO_HO2_IRR
ISOPAO2 + HO2 -> ISOPOOH	ISOPO2_HO2_IRR
MACRO2 + HO2 -> MACROOH	MACRO2_HO2_IRR
MBONO3O2 + HO2 ->	MBONO3O2_HO2_IRR
MBOO2 + HO2 -> MBOOOH	MBOO2_HO2_IRR
MEKO2 + HO2 -> MEKOOH	MEKO2_HO2_IRR
NTERPO2 + HO2 -> NTERPOOH	NTERPO2_HO2_IRR
OH + HO2 -> H2O + O2	OH_HO2_IRR
PHENO2 + HO2 -> PHENOOH	PHENO2_HO2_IRR
PO2 + HO2 -> POOH + O2	PO2_HO2_IRR
RO2 + HO2 -> ROOH	RO2_HO2_IRR
TERP2O2 + HO2 -> TERP2OOH	TERP2O2_HO2_IRR
TERPO2 + HO2 -> TERPOOH	TERPO2_HO2_IRR
TOLO2 + HO2 -> TOLOOH	TOLO2_HO2_IRR
XO2 + HO2 -> XOOH	XO2_HO2_IRR
XYLENO2 + HO2 -> XYLENOOH	XYLENO2_HO2_IRR
XYLOLO2 + HO2 -> XYLOLOOH	XYLOLO2_HO2_IRR

Table S9 Reactions used to calculate the LNOx in IRR analysis

MOZART Reactions	IRR reactions
CH3CO3 + NO2 + M -> PAN + M	CH3CO3_NO2_IRR
DICARBO2 + NO2 + M -> NDEP + M	DICARBO2_NO2_IRR
MACRO2 + NO -> .8 ONITR + nume	MACRO2_NO_a_IRR
MALO2 + NO2 + M -> NDEP + M	MALO2_NO2_IRR
MDIALO2 + NO2 + M -> NDEP + M	MDIALO2_NO2_IRR
NO2 + OH + M -> HNO3 + M	OH_NO2_IRR
PHENO + NO2 -> NDEP	PHENO_NO2_IRR

Table S10 Total OH reactivity with VOCs and NO2 and corresponding ration in Urban, Power, and Rural for April 7th (lockdown sample day). Results are for daily total (24-hours) and daytime total (10:00-17:00)

Scenario	OH+VOC		OH+NO2		(OH+VOC)/(OH+NO2)	
	Daily	**Daytime**	**Daily**	**Daytime**	**Daily**	**Daytime**
Urban						
2019BAU	46.23	40.68	10.04	8.11	4.60	5.02
2019COVID	49.26	42.63	7.93	6.17	6.21	6.91
2020BAU	18.28	15.79	4.78	3.68	3.82	4.29
2020COVID	19.55	16.71	4.02	3.01	4.86	5.55
Power						
2019BAU	19.78	17.09	7.34	5.84	2.69	2.93
2019COVID	21.92	18.96	6.56	5.22	3.34	3.63
2020BAU	11.83	10.56	5.66	4.5	2.09	2.35
2020COVID	13.19	11.78	5.11	4.05	2.58	2.91
Rural						
2019BAU	17.52	14.61	2.36	1.55	7.42	9.43
2019COVID	16.82	13.76	1.92	1.21	8.76	11.37
2020BAU	18.63	15.34	2.45	1.53	7.60	10.03
2020COVID	17.8	14.41	1.98	1.2	8.99	12.01

Table S11 The percentages of data points in each region that are in FNR transition range based on each scenario

Scenario	2019BAU	2020BAU	2020COVID
Urban grid cells	37%	36%	25%
Rural grid cells	12%	11%	6%
Power plant grid cells	36%	35%	23%

References

Granier, C., Darras, S., van der Gon, H. D., Jana, D., Elguindi, N., Bo, G., Michael, G., Marc, G., Jalkanen, J.-P., and Kuenen, J.: The Copernicus atmosphere monitoring service global and regional emissions (April 2019 version), Copernicus Atmosphere Monitoring Service, 2019.

Guttikunda, S. K., Nishadh, K., and Jawahar, P.: Air pollution knowledge assessments (APnA) for 20 Indian cities, Urban Climate, 27, 124-141, 2019.

Janssens-Maenhout, G., Crippa, M., Guizzardi, D., Dentener, F., Muntean, M., Pouliot, G., Keating, T., Zhang, Q., Kurokawa, J., and Wankmüller, R.: HTAP_v2. 2: a mosaic of regional and global emission grid maps for 2008 and 2010 to study hemispheric transport of air pollution, Atmospheric Chemistry and Physics, 15, 11411-11432, 2015.

Jena, C., Ghude, S. D., Kumar, R., Debnath, S., Govardhan, G., Soni, V. K., Kulkarni, S. H., Beig, G., Nanjundiah, R. S., and Rajeevan, M.: Performance of high resolution (400 m) PM 2.5 forecast over Delhi, Scientific reports, 11, 1-9, 2021.

Pfister, G., Wang, C. T., Barth, M., Flocke, F., Vizuete, W., and Walters, S.: Chemical Characteristics and Ozone Production in the Northern Colorado Front Range, Journal of Geophysical Research: Atmospheres, 124, 13397-13419, 2019.

Roozitalab, B., Carmichael, G. R., and Guttikunda, S. K.: Improving regional air quality predictions in the Indo-Gangetic Plain–case study of an intensive pollution episode in November 2017, Atmospheric Chemistry and Physics, 21, 2837-2860, 2021.

Vasilakos, P., Russell, A., Weber, R., and Nenes, A.: Understanding nitrate formation in a world with less sulfate, Atmos. Chem. Phys., 18, 12765-12775, 10.5194/acp-18-12765-2018, 2018.

Venkataraman, C., Brauer, M., Tibrewal, K., Sadavarte, P., Ma, Q., Cohen, A., Chaliyakunnel, S., Frostad, J., Klimont, Z., Martin, R. V., Millet, D. B., Philip, S., Walker, K., and Wang, S.: Source influence on emission pathways and ambient PM2.5 pollution over India (2015–2050), Atmos. Chem. Phys., 18, 8017-8039, 10.5194/acp-18-8017-2018, 2018.

Wang, D., Hu, J., Xu, Y., Lv, D., Xie, X., Kleeman, M., Xing, J., Zhang, H., and Ying, Q.: Source contributions to primary and secondary inorganic particulate matter during a severe wintertime PM2.5 pollution episode in Xi'an, China, Atmospheric Environment, 97, 182-194, https://doi.org/10.1016/j.atmosenv.2014.08.020, 2014.